

Cosmological constraints on parametrized interacting dark energy

R. von Marttens

Núcleo COSMO-UFES & Departamento de Física, Universidade Federal do Espírito Santo (UFES). Av. Fernando Ferrari s/n CEP 29.075-910, Vitória, ES, Brazil.

Departamento de Astronomia, Observatório Nacional, 20921-400, Rio de Janeiro, RJ, Brasil.

Département de Physique Théorique and Center for Astroparticle Physics, Université de Genève, 24 quai Ernest Ansermet, CH-1211 Geneva, Switzerland

L. Casarini

International Institute of Physics (IIP), Universidade Federal do Rio Grande do Norte (UFRN) CP 1613, 59078-970 Natal-RN, Brazil.

Institute of Theoretical Astrophysics, University of Oslo, 0315 Oslo, Norway.

D.F. Mota

Institute of Theoretical Astrophysics, University of Oslo, 0315 Oslo, Norway.

W. Zimdahl

Núcleo COSMO-UFES & Departamento de Física, Universidade Federal do Espírito Santo (UFES). Av. Fernando Ferrari s/n CEP 29.075-910, Vitória, ES, Brazil.

Abstract

We reconsider the dynamics of the Universe in the presence of interactions in the cosmological dark sector. A class of interacting models is introduced via a real function $f(r)$ of the ratio r between the energy densities of the (pressureless) cold dark matter (CDM) and dark energy (DE). The subclass of models for which the ratio r depends only on the scale factor is shown to be equivalent to unified models of the dark sector, i.e. models for which the CDM and DE components can be combined in order to form a unified dark fluid. For specific choices of the function $f(r)$ we recover several models already studied in the literature. We analyse various special cases of this type of interacting models using a suitably modified version of the CLASS

code combined with MontePython in order to constrain the parameter space with the data from supernova of type SNe Ia (JLA), the Hubble constant H_0 , cosmic chronometers (CC), baryon acoustic oscillations (BAO) and data from the Planck satellite (Planck TT). Our analysis shows that even if data from the late Universe (H_0 , SNe Ia and CC) indicate an interaction in the dark sector, the data related to the early Universe (BAO and Planck TT) constrain this interaction substantially, in particular for cases in which the background dynamics is strongly affected.

Keywords: Cosmology, dark energy and dark matter.

1. Introduction

One of the most intriguing challenges of current cosmology is the nature of the dark sector of the Universe. According to the most recent observations [1, 2, 3, 4, 5, 6, 7, 8, 9], we live in a spatially flat Universe and this dark sector contributes with approximately 95% to the cosmic substratum today. The rest of the material content of the Universe is composed by a negligible part of radiation and the remaining 4-5% by baryonic matter, the kind of matter that composes systems that interact with electromagnetic radiation, and therefore can be observed directly (like ourselves!).

Each of the components of the dark sector plays an important role in the dynamics of the Universe. The dark matter, which corresponds to 25% of the matter content of the Universe, is an exotic pressureless matter which was proposed to explain the observations of the velocity of galaxy clusters [10]. Years later, the existence of the CDM was corroborated with the studies of the rotation curves of spiral galaxies [11], which indicated that there was more mass in galaxies than could be observed through their luminosity. Moreover, the analysis of x-ray emission by galaxy clusters and gravitational lensing also indicates the presence of this exotic matter. In the context of structure formation, CDM seems to play a very important role, potentializing the growth of baryonic structures after decoupling, until they reach the non-linear regime that is currently observed ($\delta_b > 1$).

The dark energy, which is responsible for the remaining 70% of the cosmic substratum was proposed to explain the current phase of accelerated expansion of the Universe [12, 13]. Within the cosmological standard description, the DE component can be identified with the cosmological constant Λ , which *a priori* has a geometric nature in the context of the general theory of relativ-

ity. Such identification is analogous to a fluid model with a vacuum equation of state (EoS) $w = -1$ and constant energy density. As previously mentioned, this description of dark energy seems to successfully satisfy the most recent observational data, however it is in deep disagreement with the theoretical prediction for vacuum energy that comes from quantum field theory [14].

Along with the general theory of relativity (GR), the inflationary paradigm and the Big Bang nucleosynthesis (BBN), this material description composes the so-called Λ CDM model. Instead of the vacuum description, it is also common to consider a dynamical description for the DE component through a different EoS, for example, a constant EoS parameter $w \neq -1$ or some time dependent EoS parameter [15, 16]. Alternatively, several alternatives to describe the DE component are proposed in the literature, among others, the dynamical approach through a scalar field [17, 18] and modified theories of gravity [19, 20] have received much attention.

In this work, we focus on the study of cosmological models in which, unlike in the standard cosmological description, CDM and DE are not independent components, but there is a non-gravitational interaction that results in an energy exchange between them. An important feature of this class of models is that such interaction implies the existence of DE perturbations even in the case where $w = -1$. This type of models has been extensively studied in the literature [21, 22, 23, 24, 25, 26, 27, 28, 29, 30, 31, 32, 33, 34, 35, 36, 37, 38, 39] as a simple and viable alternative to the standard cosmological model, and there are arguments that indicate that it is not correct to ignore this interaction [40, 41] or to ignore the DE perturbations in dynamic DE models [42]. Recent studies indicate some remarkable observational aspects of these interacting models [43, 44, 45].

In general, the motivation for these models is phenomenological (although some cases may be based on a more fundamental argument [46]) and each model is seen completely independently of the others. Furthermore, most of the interacting models proposed in the literature are such that the interaction term is linear [47], i.e., it depends only linearly on one of the energy densities of the dark sector components. Here, we propose a more general description in which the interaction term is a real function of the energy densities of CDM and DE. This approach allows us to relate several models of interaction through a function of the ratio between the energy densities of CDM and DE. For specific cases we find analytical solutions, some of them already present in the literature.

This paper is organized as follows: In Section 2 we introduce a background description of the interaction between CDM and DE via a real function of the ratio between CDM and DE energy densities. We recover several cases already studied in the literature and we demonstrate the equivalence of a class of interacting models with unified models, i.e., models that can be described as a single perfect conservative fluid. The well-established linear perturbation theory for interacting perfect fluids is recalled in Section 3. In Section 4 we present some specific cases of interacting models obtained through the proposed generalization. In Section 5 we perform a statistical analysis for each model using the observational data from SNe Ia (JLA) [4], local measures of H_0 [48], BAO [49, 50, 51, 52, 53] and the CMB temperature anisotropy spectrum. Finally, Section 6 summarizes our results.

2. Background dynamics of interacting models

2.1. General equations

At the background level the Universe is considered to be homogeneous, isotropic and spatially flat and describable by the FLRW metric

$$ds^2 = dt^2 - a^2(t) [dr^2 + r^2 (d\theta^2 + \sin^2 \theta d\phi)], \quad (1)$$

where a is the scale factor. The expansion dynamics obeys Friedmann's equation

$$H^2 = \frac{8\pi G}{3} \rho, \quad (2)$$

and

$$\dot{H} = -4\pi G (\rho + p), \quad (3)$$

where $H \equiv \dot{a}/a$ is the Hubble rate, ρ and p are, respectively, the total energy density and the pressure of the material content of the Universe. Considering a GR context, the total cosmic fluid must be conservative,

$$\dot{\rho} + 3H (\rho + p) = 0. \quad (4)$$

We assume that the material content of the universe is composed of four components: radiation, baryons, CDM and DE, all of them described by ideal fluids with EoS $p_i = w_i \rho_i$. The radiation component will be denoted by a

subindex r and it is characterized by a state parameter $w_r = 1/3$. Baryons are a pressureless component, and will be denoted by a subindex b ($w_b = 0$). The CDM component is also pressureless, and will be denoted by a subindex c ($w_c = 0$). Lastly, the DE component will be denoted by a subindex x , it is characterized by a constant EoS parameter $w_x = -1$, which can be associated to a cosmological constant. The total energy density ρ and total pressure p are defined as the sum of contributions of all species,

$$\rho = \rho_r + \rho_b + \rho_c + \rho_x \quad \text{and} \quad p = p_r + p_x. \quad (5)$$

It is convenient to introduce the density parameters

$$\Omega_i = \frac{8\pi G}{3H^2} \rho_i, \quad (6)$$

where the index i is running over all components of the universe ($i = r, b, c, x$). Then, Friedmann's equation can be rewritten as

$$\Omega_r + \Omega_b + \Omega_c + \Omega_x = 1. \quad (7)$$

Radiation and baryons are assumed to evolve independently, their energy densities are given by

$$\dot{\rho}_r + 4H\rho_r = 0 \quad \Rightarrow \quad \rho_r = \rho_{r0} a^{-4}, \quad (8)$$

$$\dot{\rho}_b + 3H\rho_b = 0 \quad \Rightarrow \quad \rho_b = \rho_{b0} a^{-3}. \quad (9)$$

Since the nature of the dark sector is unknown, we consider a phenomenological interaction via $T_c^{\mu\nu}{}_{;\nu} = -T_x^{\mu\nu}{}_{;\nu} = Q^\mu$, where Q^μ is a four-vector and $T_c^{\mu\nu}$ and $T_x^{\mu\nu}$ are the energy-momentum tensors of CDM and DE, respectively. Because of our perfect-fluid description of CDM and DE, the spatial component of the covariant derivative of the energy-momentum tensor must be identically zero, which means that the background interaction term is characterized only by a scalar function Q , such that $Q^\mu = Qu^\mu$. Then, the background energy conservation becomes

$$\dot{\rho}_c + 3H\rho_c = -Q, \quad (10)$$

$$\dot{\rho}_x = Q. \quad (11)$$

These equations can be understood as an energy transfer between the dark components. The direction of the energy flux depends on the sign of the

scalar function Q . For $Q > 0$ we have a process of decaying CDM and DE creation, for $Q < 0$ the opposite occurs.

Here we are interested in interactions of the type $Q = 3H\gamma R(\rho_c, \rho_x)$, where γ is a dimensionless constant and R is a real function with dimension of an energy density. Using this interaction term, the energy balance equations (10) and (11) become

$$\dot{\rho}_c + 3H\rho_c \left(\gamma \frac{R}{\rho_c} + 1 \right) = 0, \quad (12)$$

$$\dot{\rho}_x - 3\gamma HR = 0. \quad (13)$$

Note that, since $R(\rho_c, \rho_x)$ is a general function of ρ_c and ρ_x , these equations are coupled. Now it is convenient to introduce the ratio r of the energy densities of CDM and DE and to consider the time evolution of this quantity,

$$r \equiv \frac{\rho_c}{\rho_x} \quad \Rightarrow \quad \dot{r} = r \left(\frac{\dot{\rho}_c}{\rho_c} - \frac{\dot{\rho}_x}{\rho_x} \right). \quad (14)$$

Combining the equations (12), (13) and (14) one obtains a differential equation for r ,

$$\dot{r} + 3Hr \left(\gamma R \frac{\rho_c + \rho_x}{\rho_c \rho_x} + 1 \right) = 0. \quad (15)$$

Equation (15) can be used to decouple equations (12) and (13) in case there exists an analytical solution $r = r(a)$. Under this condition one may find analytical solutions for ρ_c and ρ_x . To this purpose we require that the first term in the parenthesis of (15) is a function only of the ratio r , i.e.,

$$f(r) \equiv R \frac{\rho_c + \rho_x}{\rho_c \rho_x}. \quad (16)$$

Using the structure (16), equation (15) can be rewritten as

$$\dot{r} + 3Hr \left[\gamma f(r) + 1 \right] = 0. \quad (17)$$

Note that the solution of equation (17) is directly related to the cosmic coincidence problem (CCP) [54]. Any non-vanishing interaction will modify the ratio r compared to its dependence $r \propto a^{-3}$ within the Λ CDM model which is recovered for $\gamma = 0$. Interacting models have frequently been used to address the CCP (see, e.g., [24, 55, 56]). As we shall show below, the

behavior of the solution for r at $a \ll 1$ can also be used to put constraints on the interaction strength.

Here, we are interested in the class of models for which equation (17) has an analytical solution $r = r(a)$. In this case the interaction term $R(\rho_c, \rho_x)$ can be written in terms of only one of the energy densities and the scale factor,

$$R = \frac{f(r)}{1+r} \rho_c \quad \text{or} \quad R = \frac{f(r)}{1+r^{-1}} \rho_x. \quad (18)$$

Consequently, the energy balance equations (12) and (13) of the dark sector become separable,

$$\dot{\rho}_c + 3H\rho_c \left(\gamma \frac{f(r)}{1+r} + 1 \right) = 0, \quad (19)$$

$$\dot{\rho}_x - 3\gamma H\rho_x \left(\frac{f(r)}{1+r^{-1}} \right) = 0. \quad (20)$$

This encodes the first result of the paper: for interactions resulting in a ratio of the energy densities of CDM and DE which depends only on the scale factor, the individual energy balance equations are always separable.

A priori, the function $f(r)$ can be completely general, but, we assume as an *ansatz* that the interaction term has the following form,

$$Q = 3H\gamma\rho_c^\alpha\rho_x^\beta(\rho_c + \rho_x)^\sigma, \quad (21)$$

where, on dimensional grounds, the relation $\alpha + \beta + \sigma = 1$ must be satisfied. It is straightforward to see that the expression (21) corresponds to $f(r) = r^{\alpha-1}(r+1)^{\sigma+1}$. If σ is an integer, equation (21) can also be written as a power law using Newton's binomial series,

$$f(r) = r^{\alpha-1} \quad \text{if} \quad \sigma = -1, \quad (22)$$

$$f(r) = \sum_{i=0}^{|\sigma+1|} \binom{|\sigma+1|}{i} r^{\alpha-1+i} \quad \text{if} \quad \sigma \neq -1. \quad (23)$$

The same arguments can be used for interacting DE models with $w_x \neq -1$ for which the inclusion of a factor $(w_x + 1)$ in the interaction term has been proposed as a way to avoid instabilities due the DE pressure perturbations [57, 58, 59]. A similar mathematical formulation of interacting models using a function of the ratio between energy densities of CDM and DE can be found in [60].

2.2. Unified description of interacting models

An interesting feature of the class of interacting models characterized by (13) is their equivalence to unified models of the dark sector. In other words, it is possible to combine CDM and DE into a single conservative dark fluid with an EoS

$$p_d = w_d(a) \rho_d, \quad (24)$$

where the subindex d denotes the unified dark fluid. We define the energy density and the pressure of this dark fluid as a sum of the energy densities and pressures of the components,

$$\rho_d = \rho_c + \rho_x \quad \text{and} \quad p_d = p_x, \quad (25)$$

respectively. The dark-fluid energy density may be written in terms of r and only one of the energy densities ρ_c or ρ_x ,

$$\rho_d = \left(\frac{1+r}{r} \right) \rho_c \quad \text{or} \quad \rho_d = (1+r) \rho_x, \quad (26)$$

respectively. Using the second of these options, we conclude that

$$p_d = -\frac{1}{1+r} \rho_d. \quad (27)$$

This relation is completely general but the validity of equation (24) is restricted to interactions for which the ratio r depends only on the scale factor. In such a case the dark fluid satisfies the conservation equation

$$\dot{\rho}_d + 3H\rho_d \left[1 - \frac{1}{1+r(a)} \right] = 0. \quad (28)$$

Then, the Hubble rate is obtained through Friedmann's equation using only the unified dark fluid instead of the CDM and DE components separately,

$$H^2 = \frac{8\pi G}{3} (\rho_r + \rho_b + \rho_d), \quad (29)$$

where ρ_r and ρ_b are, respectively, given by equations (8) and (9), and ρ_d is the solution of equation (28). To summarize: in order to describe the background dynamics, there are two equivalent options: the first option is to choose a function $f(r)$, which means to choose a specific interaction. The second one is to start with an expression for the ratio $r(a)$, and to apply equation (28). Since $f(r)$ and $r(a)$ are related via equation (17), specifying only one of these quantities is sufficient.

3. Perturbations

3.1. Conservation equations

Restricting ourselves to scalar perturbations in a spatially flat Universe, the perturbed Robertson-Walker metric in the Newtonian gauge with the scalar degrees of freedom ψ and ϕ is given by [61],

$$ds^2 = a^2(\tau) \left[-(1 + 2\psi) d\tau^2 + (1 - 2\phi) dx^i dx_i \right], \quad (30)$$

where, for convenience, the cosmic time t was replaced by the conformal time τ .

In order to describe structure formation we have to solve the complete set of linear perturbation equations for all components of the Universe. The standard procedure to obtain the CMB temperature anisotropies is to compute the Boltzmann equations for all these components. Here we assume that baryons and radiation behave in the same way as they do in the Λ CDM model, i.e., interacting with each other via Thomson scattering before recombination but not directly with the dark sector, thus, the Boltzmann equations for these two components will be the same as the well-established equations [61]. However, since we do not have yet a microscopic description of the interaction between the dark components, corresponding Boltzmann equations are not available either. Instead, we have to use the fluid dynamical description for the components of the dark sector. Quite generally, the interaction term can be split into components parallel and orthogonal to the four-velocity,

$$Q^\mu = Qu^\mu + F^\mu, \quad F^\mu u_\mu = 0. \quad (31)$$

The background contribution of the scalar function Q already appeared in equations (10) and (11). Writing Q in the covariant form $Q = \Theta\gamma R$, its first-order part, denoted by a hat symbol, is $\hat{Q} = \hat{\Theta}\gamma R + 3H\gamma\hat{R}$. The term \hat{R} depends on the interaction model, i.e., on the energy densities of the dark sector components, the $\hat{\Theta}$ term can be obtained by linearization of the expansion scalar $\Theta \equiv u^\mu{}_{;\mu}$ about the homogeneous and isotropic background. In the Newtonian gauge it results in

$$\hat{\Theta} = \frac{1}{a} \left(\theta_{tot} - \Theta\psi - 3\phi' \right). \quad (32)$$

Here, $\theta_{tot} \equiv ik^a \partial_a v_{tot}$ where v_{tot} is related to the spatial part of the total four-velocity of the cosmic medium by $\hat{u}_{tot}^\mu = a^{-1}(-\psi, \partial^i v_{tot})$. The prime denotes a derivative with respect to the conformal time.

The ideal fluid description of the dark components implies that the first-order contribution of F^μ is purely spatial. For the total first-order interaction term we have $\hat{Q}^\mu = a \left(Q\psi + \hat{Q}, Q\hat{u}^i + F^i \right)$.

To obtain our basic set of equations we start by considering a general interacting perfect fluid with energy-momentum balance $T^{\mu\nu}_{;\nu} = Q^\mu$ and constant EoS $p = w\rho$. The first-order four-velocity of this fluid is $\hat{u}^\mu = a^{-1}(-\psi, \partial^i v)$, where v is its peculiar velocity. Introducing the density contrast $\delta \equiv \hat{\rho}/\rho$ for this fluid, where $\hat{\rho}$ is its perturbed energy density and ρ is the corresponding background quantity, as well as $\theta \equiv i k^a \partial_a v$, the well-known energy and momentum conservations in the Newtonian gauge are given by [62],

$$\begin{aligned} \delta' + 3\mathcal{H}(c_s^2 - w)\delta + 9\mathcal{H}^2(1+w)(c_s^2 - c_a^2)\frac{\theta}{k^2} + (1+w)(\theta - 3\phi') \\ = \frac{Qa}{\rho} \left[\frac{\hat{Q}}{Q} - \delta + \psi + 3\mathcal{H}(c_s^2 - c_a^2)\frac{\theta}{k^2} \right], \end{aligned} \quad (33)$$

$$\begin{aligned} \theta' + \mathcal{H}(1 - 3c_s^2)\theta - \frac{k^2 c_s^2}{1+w}\delta - k^2\psi = \frac{a}{\rho(1+w)} \left[Q\theta_{tot} - k^2\mathcal{F} \right. \\ \left. - (1 + c_s^2)Q\theta \right]. \end{aligned} \quad (34)$$

Here, $\mathcal{H} \equiv \frac{a'}{a}$ is the Hubble parameter computed with respect to the conformal time and \mathcal{F} is defined by $aF^i = \partial^i \mathcal{F}$. The quantities c_a^2 and c_s^2 correspond to the squared adiabatic and physical rest-frame sound speeds, respectively, of the fluid. Since we consider a constant EoS parameter, the adiabatic sound speed square c_a^2 coincides with w . In order to avoid instabilities, the physical sound speed square c_s^2 of dynamical DE has to be non-negative, Here, we follow the quintessence motivation [58, 63, 62] and we assume $c_s^2 = 1$.

Now we apply the general equations (33) and (34) to each of the dark components. For the CDM component we have,

$$\dot{\delta}_c + \theta_c - 3\dot{\phi} = \frac{aQ}{\rho_c} \left(\delta_c - \frac{\hat{Q}}{Q} - \psi \right), \quad (35)$$

$$\dot{\theta}_c + \mathcal{H}\theta_c - k^2\psi = \frac{aQ}{\rho_c} (\theta_{tot} - \theta_c). \quad (36)$$

Since $w_x = -1$, the velocity θ_x of the DE component has no dynamics. The

energy balance is

$$\dot{\delta}_x + 3\mathcal{H}(c_s^2 + 1)\delta_x = -\frac{aQ}{\rho_x} \left(\delta_x - \frac{\hat{Q}}{Q} \right). \quad (37)$$

Note that even if $w_x = -1$ the DE component agglomerates. According the equation (37) fluctuations of the DE component can have two sources: the first one is the non-adiabatic character of interacting DE, which leads to a physical sound speed different from the adiabatic sound speed (in this case, different from -1). Indeed, the non-adiabaticity can play an important role at the linear level [64]. The second one is the interaction term on the right-hand side of equation (37). In order to solve the set of equations (35), (36) and (37), we use the well-established adiabatic initial conditions for interacting models [63].

4. Specific interacting DE models

In the most general case, equation (15) with (22) and (23) has no tractable analytical solution. For specific functions $f(r)$, however, solutions can be found. For some simple choices of $f(r)$ we shall recover models that have been previously studied in the literature. The interacting models will be called as IDEM (Interacting Dark Energy Model) followed by a number that will identify each model.

4.1. IDEM 1: $f(r) = 1$

The simplest non-vanishing function is $f(r) = 1$, which corresponds to the case $\alpha = \beta = 1$ in (22). This parametrization leads to an interaction term

$$Q = 3H\gamma \frac{\rho_c \rho_x}{\rho_c + \rho_x}. \quad (38)$$

This interaction term coincides exactly with that of a decomposed generalized Chaplygin gas model [65, 66, 67]. With (38) equation (17) for r can be solved to yield

$$r(a) = r_0 a^{-3(\gamma+1)}, \quad (39)$$

which recovers the corresponding expression in [68]. Note that, with the reasonable physical assumption that the interaction it is not too strong, i.e., $|\gamma| < 1$, the asymptotic behavior of $r(a)$ is the same as in the Λ CDM model: if $a \rightarrow 0$ then $r(a) \rightarrow \infty$, which means a CDM domination over DE at early

times; if $a \rightarrow \infty$ then $r(a) \rightarrow 0$, which means a DE domination over CDM in the far future.

Figure 1 shows the solution of $r(a)$ for different values of γ . For negative values of the interaction parameter ($\gamma < 0$) the ratio $r(a)$ reaches the order of 1 earlier than in the standard model ($\gamma = 0$). In this sense, the CCP may be considered alleviated for $\gamma < 0$.

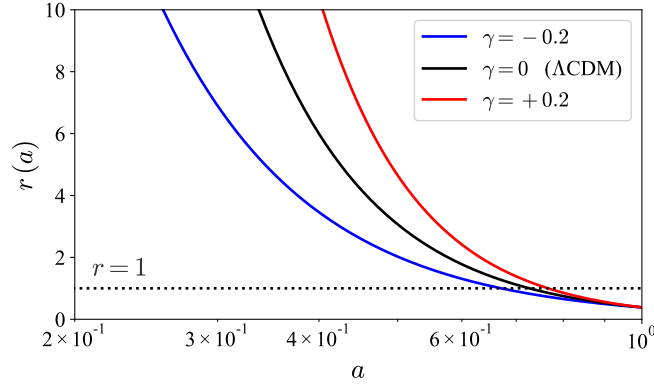


Figure 1: Ratio $r(a)$ between CDM energy density and DE energy density for IDEM 1.

The background solutions for the CDM and DE energy densities can be obtained solving the equations (12) and (13), which leads to,

$$\rho_c = \rho_{c0} a^{-3} \left(\frac{\Omega_{c0} + \Omega_{x0} a^{3(\gamma+1)}}{\Omega_{c0} + \Omega_{x0}} \right)^{-\frac{\gamma}{\gamma+1}}, \quad (40)$$

$$\rho_x = \rho_{x0} a^{-3(1+\gamma+1)} \left(\frac{\Omega_{c0} + \Omega_{x0} a^{-3(\gamma+1)}}{\Omega_{c0} + \Omega_{x0}} \right)^{-\frac{\gamma}{\gamma+1}}. \quad (41)$$

With these energy densities of the dark sector components, Friedmann's equation (2) provides us with the Hubble rate square

$$H^2 = H_0^2 \left[(\Omega_{c0} + \Omega_{x0}) \left(\frac{\Omega_{c0} + \Omega_{x0} a^{3(\gamma+1)}}{\Omega_{c0} + \Omega_{x0}} \right)^{\frac{1}{1+\gamma}} a^{-3} + \Omega_{b0} a^{-3} + \Omega_{r0} a^{-4} \right]. \quad (42)$$

In order to quantify the effect of the interaction on the background solutions it is convenient to analyze the density parameter $\Omega_i(a) = \rho_i/\rho_{cr}$, where

ρ_{cr} is the critical density, defined as $\rho_{cr} = 3H^2/8\pi G$. Figure 2 shows the density parameters for all components of the Universe using different values of γ . According to figure 2, negative values for the interaction parameter ($\gamma < 0$) delay the equivalence between radiation and matter (CDM + baryons). They also reduce the CDM component and increase the baryonic component during matter domination. Positive values for the interaction parameter ($\gamma > 0$) do the opposite. The existence of DE perturbations and the shift of the era of equivalence have notable and well-known impacts on the physics of the CMB anisotropies. While the DE perturbations mainly affect large scales of the CMB spectrum, a change of the era of equivalence considerably alters the radiation driving of the acoustic peaks and changes the balance between CDM and baryonic matter, leading to a different baryon loading [66, 67]. In addition, it is expectable that a non-vanishing γ affects the distribution of matter inhomogeneities since the time of equivalence between radiation and matter is directly related to the location of the peak of the linear matter power spectrum and to the BAO imprint on it.

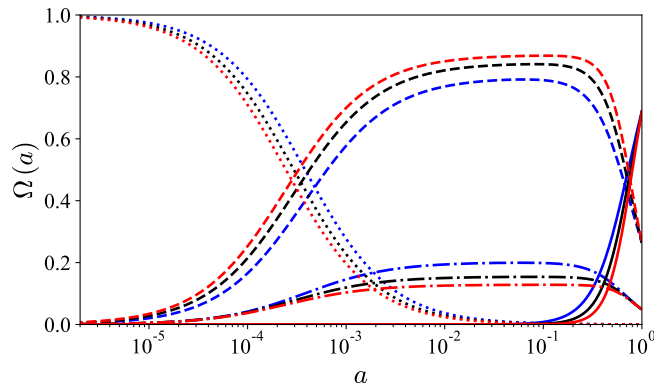


Figure 2: Density parameters for all components of the Universe for IDEM 1. The solid lines correspond to the DE component, the dashed lines to CDM, the dot-dashed lines to the baryonic component and the dotted lines to radiation. Different interaction parameters are distinguished by different colors: blue for $\gamma = -0.2$, black for $\gamma = 0$ (non-interacting case), and red for $\gamma = +0.2$.

The equivalent unified dark-sector model is described through the quan-

titles w_d and ρ_d , for which we find

$$w_d(a) = -\frac{\Omega_{x0}}{\Omega_{x0} + \Omega_{c0} a^{-3(\gamma+1)}} \quad \text{and} \quad \rho_d = \rho_{d0} a^{-3} \left(\frac{a^{3(\gamma+1)} + r_0}{1 + r_0} \right)^{\frac{1}{1+\gamma}}, \quad (43)$$

respectively. Figure 3 shows the evolution of the effective dark EoS parameter for different values of γ . In the past the unified dark fluid behaves like CDM (when $a \rightarrow 0$ we have $w_d \rightarrow 0$), and currently the value for w_d is negative. Since $a \rightarrow \infty$ leads to $r \rightarrow 0$, the dark EoS parameter tends to $w_d = -1$ in the far-future limit.

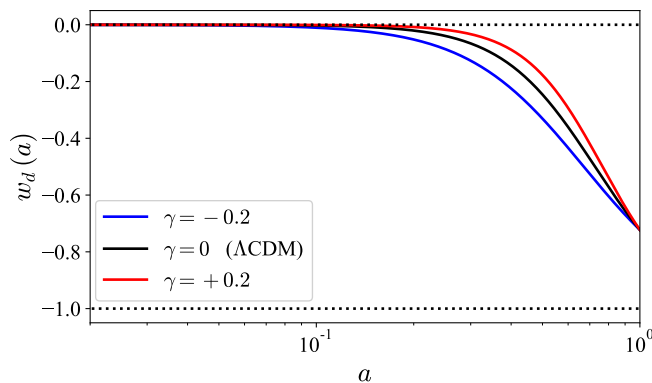


Figure 3: EoS parameter for the unified description of IDEM 1.

Recalling that in the background the expansion scalar Θ reduces to $\Theta = 3H$, the interaction term (38) can be seen as a covariant scalar quantity. Then, its first-order perturbation is

$$\hat{Q} = Q \left(\frac{\hat{\Theta}}{\Theta} + \frac{\rho_c \delta_x + \rho_x \delta_c}{\rho_c + \rho_x} \right). \quad (44)$$

This completes our description of the IDEM 1.

4.2. *IDEM 2*: $f(r) = \frac{1}{r}$

The second case studied is $f(r) = 1/r$. It is obtained from (22) with $\alpha = 0$ and $\beta = 2$, equivalent to an interaction term

$$Q = 3H\gamma \frac{\rho_x^2}{\rho_c + \rho_x}. \quad (45)$$

A statistical analysis of this model using SNe Ia data was performed in [69]. From equation (15) we obtain for $r(a)$,

$$r(a) = r_0 a^{-3} - \gamma (1 - a^{-3}) . \quad (46)$$

This solution has an interesting asymptotic behavior. In the early universe, when a tends to zero, the ratio between CDM and DE energy densities goes to $(r_0 + \gamma) a^{-3}$ i.e., it diverges. This limit means that CDM always dominates over DE in the past, but, if $\gamma < -r_0$, the DE density arises from an initial negative regime. In the following we shall exclude such primordial negative DE density phase by imposing the constraint $\gamma > -r_0$. In the far future, i.e., when $a \gg 1$, solution 46 tends to $-\gamma$, i.e., a certain amount of CDM will persist forever. Furthermore, this limit implies that for a positive interaction parameter the DE density will become negative in the future. Figure 4 shows the ratio $r(a)$ for IDEM 2 for different values of γ . Again, negative values of the interaction parameter ($\gamma < 0$) can alleviate the CCP. Equation (20)

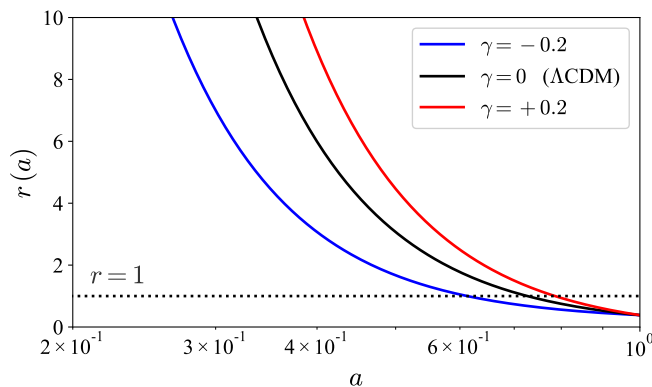


Figure 4: Ratio between CDM energy density and DE energy density $r(a)$ for IDEM 2.

provides us with the background DE energy density

$$\rho_x = \rho_{x0} a^{-\frac{3\gamma}{\gamma-1}} \left[\frac{(1-\gamma)\Omega_{x0} + a^{-3}(\Omega_{c0} + \gamma\Omega_{x0})}{(\Omega_{c0} + \Omega_{x0})} \right]^{-\frac{\gamma}{\gamma-1}} . \quad (47)$$

The CDM energy density is found by combining (47) with (46). Then, the background dynamics is completely known. Figure 5 shows the density parameters for all components for different values of γ . Obviously, the behavior of the background solutions for IDEM 2 is very similar to that of IDEM 1.

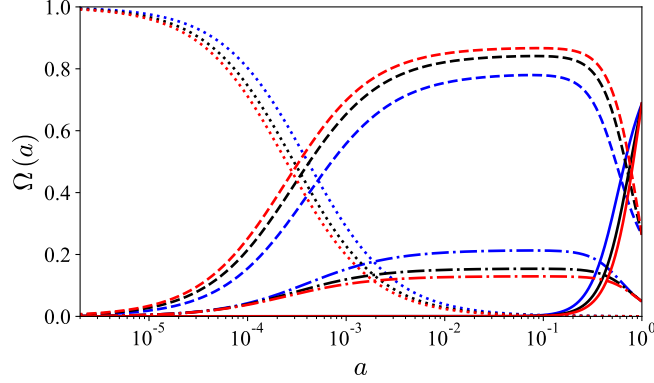


Figure 5: Density parameters for all components of the Universe for IDEM 2. The solid lines correspond to DE, the dashed lines to CDM, the dot-dashed lines to baryons and the dotted lines to radiation. Curves in blue refer to $\gamma = -0.2$, curves in black to $\gamma = 0$ (non-interacting case) curves in red to $\gamma = +0.2$.

The unified model of the dark sector is determined by the combination of equations (27) and (46). The effective dark EoS parameter is shown in figure 6. It is also very similar to that of model IDEM 1.

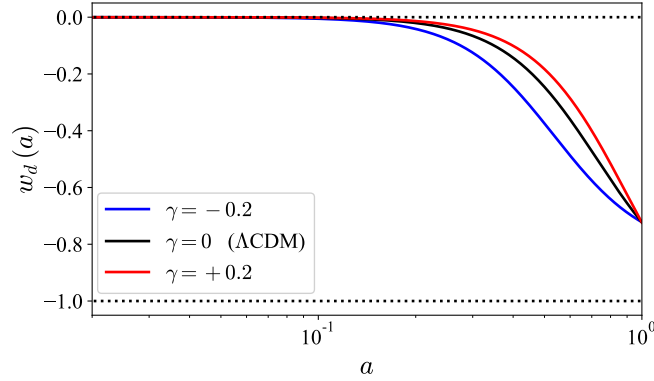


Figure 6: EoS parameter for the unified description of model IDEM 2.

Finally, at linear order the interaction parameter (45) is

$$\hat{Q} = Q \left(\frac{\hat{\Theta}}{\Theta} + \frac{\rho_x \delta_x + 2\rho_c \delta_x - \rho_c \delta_c}{\rho_c + \rho_x} \right). \quad (48)$$

4.3. IDEM 3: $f(r) = r$

The choice $f(r) = r$ is realized for $\alpha = 2$ and $\beta = 0$ in (22). It leads to the interaction parameter

$$Q = 3H\gamma \frac{\rho_c^2}{\rho_c + \rho_x}. \quad (49)$$

A statistical analysis with SNe Ia data for this model was also performed in [69]. With $f(r) = r$ equation (15) yields

$$r(a) = r_0 \frac{a^{-3}}{1 + r_0\gamma - r_0\gamma a^{-3}}. \quad (50)$$

In the early-universe limit, i.e. for $a \ll 1$, the ration between CDM and DE energy densities tends to $-1/\gamma$. Since we wish to avoid an early negative DE density phase again, we require the interaction parameter to be negative. For $a \gg 1$, independently of the value of γ , the ratio $r(a)$ tends to zero. Figure 7 shows $r(a)$ for $\gamma = -0.2$ and $\gamma = 0$. It is evident that for a non-vanishing $\gamma < 0$ the ratio between CDM and DE energy densities does not diverge for $a \ll 1$. In a sense, an interactions of this type may solve the CCP. Equation

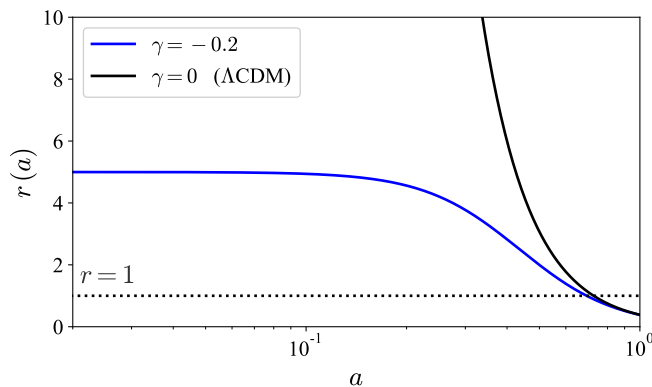


Figure 7: Ratio $r(a)$ between CDM energy density and DE energy for IDEM 3.

(19) for the CDM energy density results in

$$\rho_c = \rho_{c0} a^{-3} \left[\frac{\gamma\Omega_{c0} + (1 - \gamma)\Omega_{c0}a^{-3} + \Omega_{x0}}{(\Omega_{c0} + \Omega_{x0})} \right]^{-\frac{\gamma}{\gamma-1}}. \quad (51)$$

The corresponding DE energy density follows from (51) with (46). Figure 8 shows the density parameters for all components for different values of γ . As one can see, even a small value of the interaction parameter can modify drastically the background evolution of all components of the universe and, consequently, the entire expansion history. For this reason it is expectable that the data will strongly constrain the interaction parameter for IDEM 3.

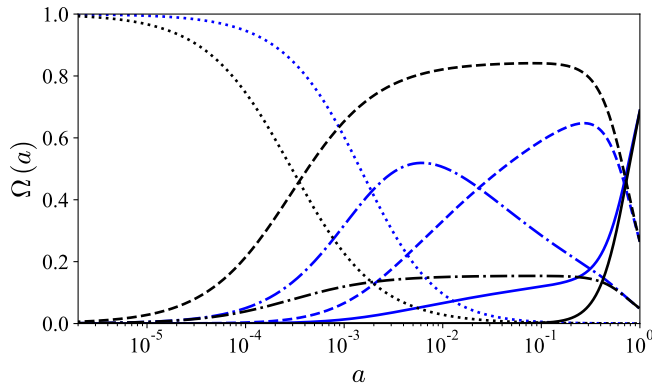


Figure 8: Density parameter for all components of the Universe for IDEM 3. The solid lines correspond to DE, the dashed lines to CDM, the dot-dashed lines to the baryonic component and the dotted lines to radiation. The blue curves refer to $\gamma = -0.2$ and the black ones to $\gamma = 0$ (non-interacting case).

The effective dark EoS parameter in figure 9 is obtained by combining equations (27) and (50). The value of $|\gamma|$ quantifies the deviation from pure matter domination in the early universe.

The first-order interaction parameter of model IDEM 3 becomes

$$\hat{Q} = Q \left(\frac{\hat{\Theta}}{\Theta} + \frac{\rho_c \delta_c + 2\rho_x \delta_c - \rho_x \delta_x}{\rho_c + \rho_x} \right). \quad (52)$$

4.4. IDEM 4: $f(r) = 1 + \frac{1}{r}$

With $\alpha = 0$, $\beta = 1$ and $\sigma = 0$ in (23) one has $f(r) = 1 + 1/r$ and

$$Q = 3H\gamma\rho_x. \quad (53)$$

From (15), one finds the ratio $r(a)$,

$$r(a) = a^{-3\gamma} \frac{(r_0 a^{-3} + \gamma a^{-3} - \gamma a^{3\gamma} + r_0 \gamma a^{-3})}{1 + \gamma}. \quad (54)$$

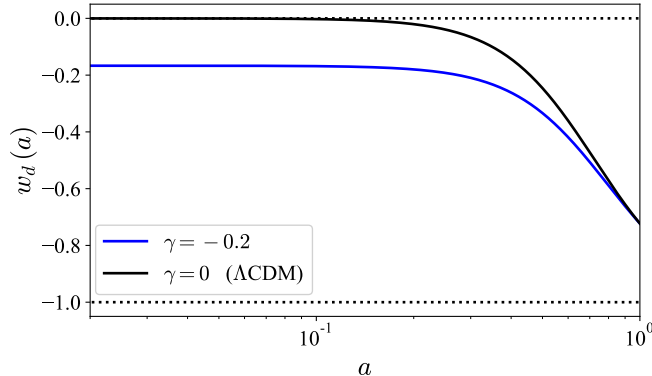


Figure 9: EoS parameter for the unified description of model IDEM 3. The blue lines correspond to $\gamma = -0.2$, the black lines correspond to $\gamma = 0$ (non-interacting case).

In the early universe, when a tends to zero, the ratio $r(a)$ diverges, i.e., CDM always dominates. The sign of $r(a)$ in this limit is determined by the combination $[\gamma + r_0(1 + \gamma)]$. For $\gamma < -r_0/(1 + r_0)$ DE arises from a negative DE density regime. To exclude an early negative DE density phase we shall restrict ourselves to $\gamma > -r_0/(1 + r_0)$ which puts a negative lower bound on the value of the interaction parameter. In the far future, i.e., for $a \gg 1$, the solution (54) tends to $-\gamma/(1 + \gamma)$, which means that there is a remaining CDM component that exists forever. As for IDEM 2, a positive γ leads to negative DE density in the future.

Figure 10 shows the ratio $r(a)$ for the IDEM 4 model for different values of γ . Just like IDEM 1 and IDEM 2, negative values of the interaction parameter ($\gamma < 0$) can alleviate the CCP. From equation (20) the background DE density for this model is

$$\rho_x = \rho_{x0} a^{3\gamma}. \quad (55)$$

Together with (54) it determines the background dynamics. Figure 11 shows the density parameters for all components for different values of γ . The background dynamics of model IDEM 4 is very similar to the dynamics of the previously studied models IDEM 1 and IDEM 2. The effective unified dark fluid EoS parameter which follows from (27) with (54) is shown in Figure 12. It is also very similar to the EoS parameters of models IDEM 1 and IDEM 2. The linear-order expression for the interaction parameter,

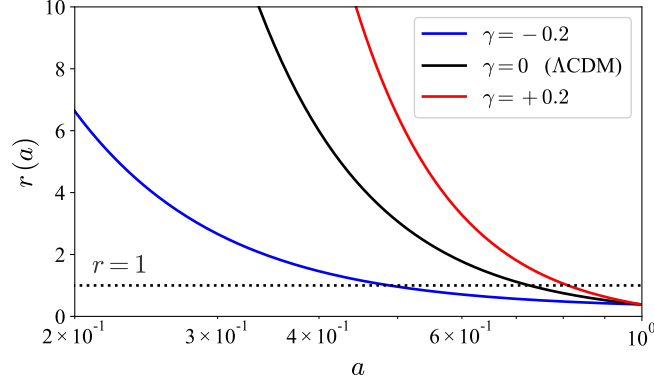


Figure 10: Ratio $r(a)$ between CDM energy density and DE density for IDEM 4.

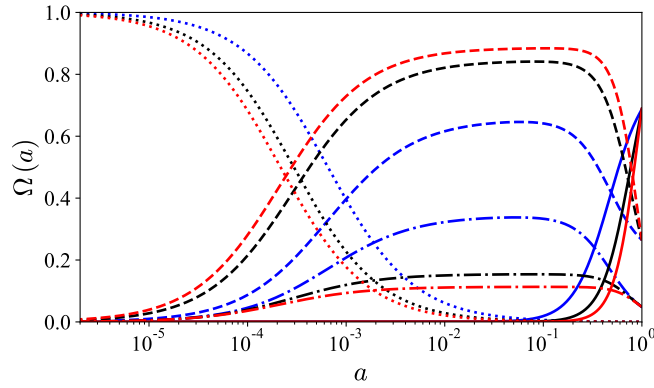


Figure 11: Density parameters for all components of the Universe for IDEM 4. The solid lines correspond to DE, the dashed lines to CDM component, the dot-dashed lines to baryons and the dotted lines to the radiation component. The blue color denotes the case $\gamma = -0.2$, the black curves refer to $\gamma = 0$ (non-interacting case) and the red ones to $\gamma = +0.2$.

calculated from (53), is

$$\hat{Q} = Q \left(\frac{\hat{\Theta}}{\Theta} + \delta_x \right). \quad (56)$$

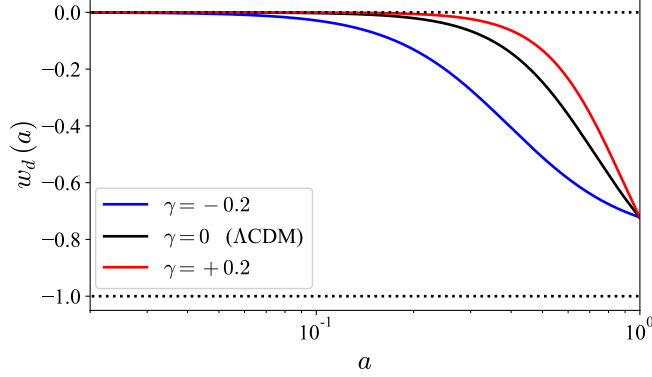


Figure 12: EoS parameter for the unified description of IDEM 4.

4.5. IDEM 5: $f(r) = 1 + r$

Equation (23) with $\alpha = 1$, $\beta = 0$ and $\sigma = 0$ results in $f(r) = 1 + r$ and in

$$Q = 3H\gamma\rho_c \quad (57)$$

for the interaction parameter. The solution of equation 15 is

$$r(a) = -\frac{1 + \gamma}{\gamma - a^{3(1+\gamma)} \left(\frac{1 + \gamma + r_0\gamma}{r_0} \right)}. \quad (58)$$

For $a \ll 1$ the ratio r tends to $-(1 + \gamma)/\gamma$, where the relation $\gamma > -1$ must be satisfied. Excluding again an initial negative DE density phase, we restrict our analysis to negative values of γ with $|\gamma| < 1$. For $a \gg 1$ the ratio $r(a)$ tends to zero. Figure 13 shows $r(a)$ for $\gamma = -0.2$ and $\gamma = 0$. For $\gamma = -0.2$ the ratio between CDM and DE densities does not diverge for $a \ll 1$ which is a similar feature as already found for model IDEM 3. Equation (19) yields

$$\rho_c = \rho_{c0} a^{-3(1+\gamma)}, \quad (59)$$

such that the background dynamics is fixed together with (46). Figure 14 shows the density parameters for $\gamma = -0.2$ and $\gamma = 0$. As in model IDEM 3, already a small non-vanishing interaction parameter can substantially modify the background evolution of all the components. From (27) and (58) one finds the effective unified dark EoS parameter visualized in Figure 15. Similar to

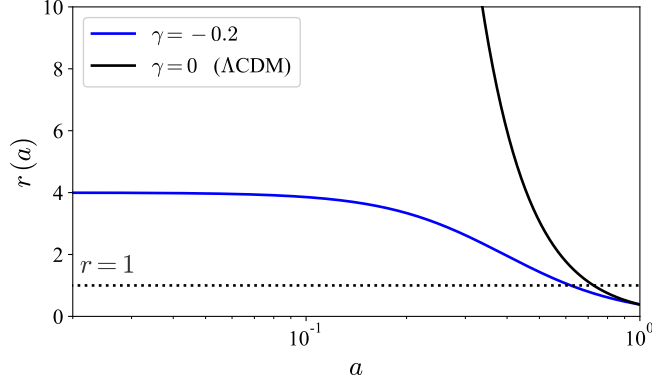


Figure 13: Ratio $r(a)$ between CDM energy density and DE density for IDEM 5.

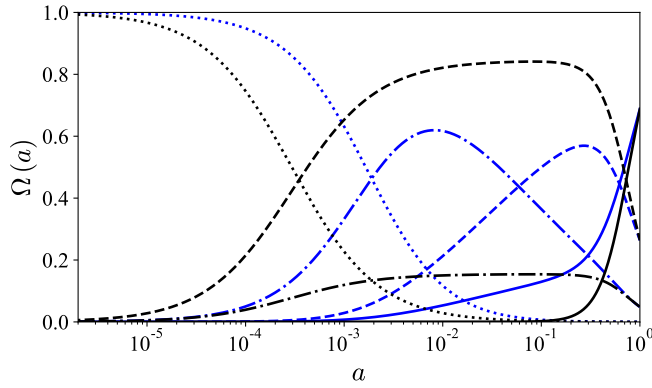


Figure 14: Density parameters for all components of the Universe for IDEM 5. The solid lines correspond to DE, the dashed lines to CDM, the dot-dashed lines to baryonic matter and the dotted lines to the radiation component. Blue curves refer to $\gamma = -0.2$ and black curves to $\gamma = 0$ (non-interacting case).

model IDEM 3, the absolute value $|\gamma|$ quantifies the difference to the EoS for pressureless matter at $a \ll 1$. The linearized interaction parameter for this model is given by

$$\hat{Q} = Q \left(\frac{\hat{\Theta}}{\Theta} + \delta_c \right). \quad (60)$$

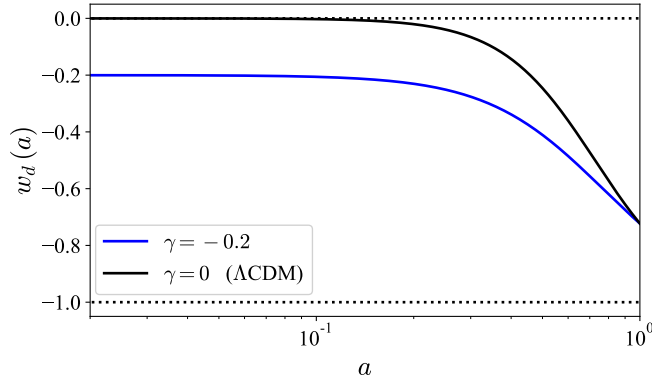


Figure 15: EoS parameter for the unified description of IDEM 5.

4.6. Interaction time evolution

Our analysis reveals that the five investigated models can be divided into two groups. The first group, comprised by IDEM 1, IDEM 2 and IDEM 4, is characterized by interactions which become dynamically relevant only recently, i.e., close to the present time. Technically, this is related to the proportionality of the interaction term to (a power of) the DE density. The cosmological dynamics at high redshift is almost unaffected and coincides with that of the standard model. The second group is made up of IDEM 3 and IDEM 5. Here, the interaction term is proportional to (a power of) the CDM energy density which means it is relevant already at early times. Fig. 16 shows the temporal evolution for all five models with $\gamma = -0.2$ (left panel) and $\gamma = +0.2$ (right panel). At late times all models behave similarly, but at early times IDEM 3 and IDEM 5 differ strongly from the other models. Fig. 16 demonstrates that, even though $|Q|$ values of IDEM 1 and IDEM 4 are growing at high redshift, at $z \approx 10^4$ the $|Q|$ values for the models IDEM 3 and IDEM 5 are about eight orders of magnitude larger. In turn, IDEM 2 presents much lower values of $|Q|$ compared to the other models at recombination era.

5. Statistical analysis

In this section we present a statistical analysis for the IDEMs presented in the previous sections. The statistical analysis was performed through a

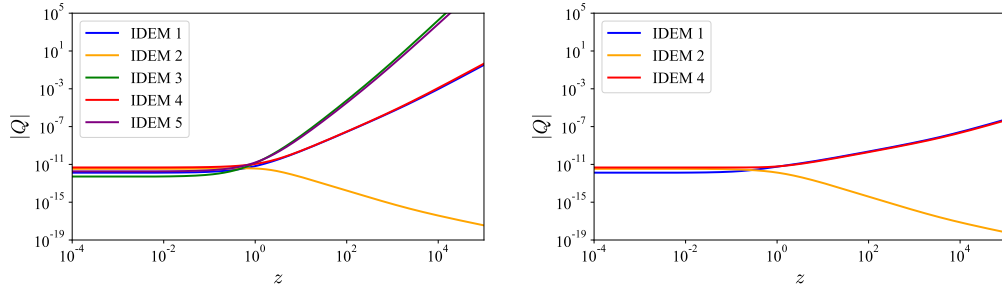


Figure 16: Interaction parameter for all the 5 models. Left panel: Negative interaction parameter ($\gamma = -0.2$). Right panel: Positive interaction parameter ($\gamma = +0.2$).

suitable modification of the Boltzmann code CLASS [70] and the MCMC statistical code MontePython [71, 72].

5.1. Observational data

In order to understand how each of the data sets constrains an interaction in the dark sector, the statistical analysis is performed gradually. At first we use geometrical tests related only to the recent expansion history of the Universe: Type-Ia Supernovae (SNe Ia), the present value of the Hubble rate (H_0) and Cosmic Chronometers (CC). Thereafter, we add Baryonic Acoustic Oscillations (BAO) data which, while representing a geometrical test, are related to the primordial photon-baryon fluid. Finally, we constrain the models using the Planck TT data. We start by introducing the data sets used in the statistical analysis and their respective likelihoods.

Type-Ia Supernovae (SNe Ia): The first data set used to perform statistical analysis is the SNe Ia data. Historically, the SNe Ia were of great importance for cosmology, having been the key observation of the accelerated expansion observed currently [12, 13]. In this work, we use the complete set of the “Joint Light-curve Analysis” (JLA) sample [4], which contains 740 data points from $z = 0.01$ until $z = 1.30$ ¹. The observable quantity in this case is the distance modulus

$$\mu^{obs.} = m_B^* + \alpha x_1 - \beta c - \mathcal{M}_B, \quad (61)$$

¹The data is available in http://supernovae.in2p3.fr/sdss_snls_jla/jla_likelihood_v6.tgz.

where m_B^* is the B -band peak magnitude measured in the rest-frame, x_1 is the time stretching of the light curve at maximum brightness, c is the color of the SN at maximum brightness and \mathcal{M} is related to the absolute B -band magnitude. The parameter \mathcal{M}_B depends on the host stellar mass,

$$\mathcal{M}_B = \begin{cases} M & \text{if } M_{\text{stellar}} \leq 0, \\ M + \Delta_M & \text{otherwise.} \end{cases} \quad (62)$$

On the other hand, from a theoretical point of view, the distance modulus, in units of Mpc, can be obtained as

$$\mu^{\text{th.}} = 5 \log \left[(z + 1) \int_0^z \frac{dz'}{E(z')} \right] + 25, \quad (63)$$

where the term in square brackets is the luminosity distance. The statistical analysis is then performed using the equations (61) and (63) to write the likelihood function,

$$2 \ln (\mathcal{L}_{\text{SNe}}) = \Delta \vec{\mu}^T \mathcal{C}_{JLA}^{-1} \Delta \vec{\mu}, \quad (64)$$

where $\Delta \vec{\mu}$ is a vector whose components are $\mu_i^{\text{obs.}} - \mu^{\text{th.}}(z_i)$ and \mathcal{C}_{JLA} is the covariance matrix of the JLA data, which is given by the sum of a statistical part and a systematic part ($\mathcal{C}_{JLA} = \mathcal{C}_{\text{stat.}} + \mathcal{C}_{\text{sys.}}$).

Current value of the Hubble rate (H_0): As the second observable quantity, we use the recent model independent measure of the local value of the Hubble parameter from [73]. Since SNe Ia can not constrain simultaneously the parameters M and H_0 , we consider a combination of SNe Ia with this data point of H_0 . The likelihood function in this case is

$$2 \ln (\mathcal{L}_{H_0}) = \left(\frac{H_0 - 73.24}{1.74} \right)^2. \quad (65)$$

Cosmic Chronometers (CC): The third data set refers to the so-called cosmic chronometers. These are also model-independent data which are obtained from measures of differential ages of old galaxies that evolve passively at different times (different values of redshift, from $z = 0.07$ until $z = 1.75$). Combining these measures with the known redshift of the galaxy, one obtains the Hubble rate at the time. In this work we use the 31 data points presented in table 1.

Since all data points are independent, the likelihood function is given by,

$$2 \ln (\mathcal{L}_{H(z)}) = \sum_{i=1}^{31} \left[\frac{H^{(i)} - H(z^{(i)})}{\sigma_{H(z)}^{(i)}} \right]^2. \quad (66)$$

| z | $H(z)$ | $\sigma_{H(z)}$ | Ref. | z | $H(z)$ | $\sigma_{H(z)}$ | Ref. | z | $H(z)$ | $\sigma_{H(z)}$ | Ref. |
|--------|--------|-----------------|------|--------|--------|-----------------|------|-------|--------|-----------------|------|
| 0.07 | 69.0 | 19.6 | [74] | 0.4 | 95.0 | 17.0 | [75] | 0.875 | 125.0 | 17.0 | [76] |
| 0.09 | 69.0 | 12.0 | [75] | 0.4004 | 77.0 | 10.2 | [77] | 0.88 | 90.0 | 40.0 | [78] |
| 0.12 | 68.6 | 26.2 | [74] | 0.4247 | 87.1 | 11.2 | [77] | 0.9 | 117.0 | 23.0 | [75] |
| 0.17 | 83.0 | 8.0 | [75] | 0.4497 | 92.8 | 12.9 | [77] | 1.037 | 154.0 | 20.0 | [76] |
| 0.179 | 75.0 | 4.0 | [76] | 0.47 | 89.0 | 49.6 | [79] | 1.3 | 168.0 | 17.0 | [75] |
| 0.199 | 75.0 | 5.0 | [76] | 0.4783 | 80.9 | 9.0 | [77] | 1.363 | 160.0 | 33.6 | [80] |
| 0.2 | 72.9 | 29.6 | [74] | 0.48 | 97.0 | 62.0 | [78] | 1.43 | 177.0 | 18.0 | [75] |
| 0.27 | 77.0 | 14.0 | [75] | 0.593 | 104.0 | 13.0 | [76] | 1.53 | 140.0 | 14.0 | [75] |
| 0.28 | 88.8 | 36.6 | [74] | 0.68 | 92.0 | 8.0 | [76] | 1.75 | 202.0 | 40.0 | [75] |
| 0.352 | 83.0 | 14.0 | [76] | 0.781 | 105.0 | 12.0 | [76] | 1.965 | 186.0 | 50.4 | [80] |
| 0.3802 | 83.0 | 13.5 | [77] | | | | | | | | |

Table 1: Cosmic chronometers data.

Baryonic Acoustic Oscillations (BAO): The fourth data set used comes from the analysis of the baryonic acoustic oscillations. Even if the BAO have a perturbative nature, they produce an imprint on the galaxy distribution that can be measured using background quantities. The relevant physical quantities for the BAO data are the sound horizon at the drag time, the angular distance and the spherically-averaged distance, which are given respectively by,

$$r_s \equiv \int_0^{a_{\text{drag}}} \frac{c_s(a)}{Ha^2} da, \quad (67)$$

$$D_A(z) = \frac{1}{1+z} \int_0^z \frac{d\tilde{z}}{H(\tilde{z})}, \quad (68)$$

$$D_V(z) = \left[(1+z)^2 D_A^2(z) \frac{z}{H(z)} \right]^{1/3}, \quad (69)$$

where, in equation (67), c_s corresponds to the sound speed in the primordial photon-baryon plasma. Table 2 shows all the data used in this work with the respective surveys from where the data was obtained.

In general, the BAO likelihood takes the following form,

$$2 \ln(\mathcal{L}_{BAO}) = \Delta \vec{V}^T \mathcal{C}_{BAO}^{-1} \Delta \vec{V}. \quad (70)$$

In the above equation, $\Delta \vec{V}$ is a vector whose components are given by $V_i^{obs.} - V_i^{th.}(z_i)$, where V corresponds to the BAO variables in the third column of table 2, and \mathcal{C}_{BAO} is the covariance matrix of the data. In this case, only the data from WiggleZ and BOSS-DR12 are correlated, and their respective

| Catalog | z | BAO variable | BAO measurement | σ_{BAO} | r_s^{fid} | Ref. |
|--------------|-------|---|--------------------|-----------------|-------------|------|
| 6dFGS | 0.106 | $\frac{r_s}{D_V}$ | 0.327 | 0.015 | * | [49] |
| SDSS DR7 MGS | 0.15 | $D_V \frac{r_s^{fid}}{r_s}$ | 4.47 | 0.16 | 148.69 | [50] |
| BOSS-LOWZ | 0.32 | $D_V \frac{r_s^{fid}}{r_s}$ | 8.47 | 0.17 | 149.28 | [51] |
| BOSS-DR12 | 0.38 | $D_A(1+z) \frac{r_s^{fid}}{r_s}$ $H \frac{r_s^{fid}}{r_s}$ | 1512.39 81.2087 | 25.00 2.3683 | 147.78 | [52] |
| | 0.51 | $D_A(1+z) \frac{r_s^{fid}}{r_s}$ $H \frac{r_s^{fid}}{r_s}$ | 1975.22 90.9029 | 30.10 2.3288 | | |
| | 0.61 | $D_A(1+z) \frac{r_s^{fid}}{r_s}$ $H \frac{r_s^{fid}}{r_s}$ | 2306.68 98.9647 | 37.08 2.5019 | | |
| WiggleZ | 0.44 | $D_V \frac{r_s^{fid}}{r_s}$ | 1716 | 83 | 148.6 | [53] |
| | 0.60 | | 2221 | 101 | | |
| | 0.73 | | 2516 | 86 | | |
| BOSS-CMASS | 0.57 | $D_V \frac{r_s^{fid}}{r_s}$ | 13.77 | 0.13 | 149.28 | [51] |

Table 2: BAO data.

covariance matrices are

$$\mathcal{C}_{WiggleZ}^{-1} = 10^{-4} \begin{pmatrix} 2.17898878 & -1.11633321 & 0.46982851 \\ & 1.70712004 & -0.71847155 \\ & & 1.65283175 \end{pmatrix} \quad (71)$$

$$\mathcal{C}_{BOSS-DR12} = 10^4 \begin{pmatrix} 624.707 & 23.729 & 325.332 & 8.34963 & 157.386 & 3.57778 \\ & 5.60873 & 11.6429 & 2.33996 & 6.39263 & 0.968056 \\ & & 905.777 & 29.3392 & 515.271 & 14.1013 \\ & & & 5.42327 & 16.1422 & 2.85334 \\ & & & & 1375.12 & 40.4327 \\ & & & & & 6.25936 \end{pmatrix} \quad (72)$$

Recently, a statistical analysis using data from angular BAO was performed in [81].

Planck TT: The last data set used to constrain the interacting models is the Planck measurements of the CMB temperature anisotropy. As it is well-know, the CMB data is able to provide a strong constraint on the parameter Ω_{c0} , then, since the interaction parameter γ affects the CDM dynamics (as well as the DE dynamics), it is also expected that the CMB data can strongly constrain the interacting models. In this work, we use the Commander and Plik codes ², respectively, for the low l analysis ($l < 30$), and for the high l

²Both, likelihood code and data, are available in <http://pla.esac.esa.int/pla/#cosmology>.

analysis ($l \geq 30$) [82].

5.2. Results

Our results are summarized in tables 3 and 4, and figures 17, 18, 19, 20, and 21. In table 3 we list the values for H_0 , Ω_{m0} and γ where Ω_{m0} is the total matter density parameter, defined by the sum of CDM and baryon contributions. For the background tests the baryon density parameter was fixed by the results from nucleosynthesis [83], in the Planck TT analysis, however, Ω_{b0} is a free parameter. Table 4 shows the results for $\Omega_{b0}h^2$, $\Omega_{c0}h^2$, the actual angular scale of the sound horizon at decoupling $100\theta_s$, the spectral tilt n_s and the reionization parameter τ_{reio} if only the Planck TT data are used. We mention that for all tests, the Gelman-Rubin convergence parameter satisfies the condition $\hat{R} - 1 < 0.01$ [84].

| Model | Data | H_0 | Ω_{m0} | γ | χ^2_{min} |
|-------|-----------------------|-------------------------|------------------------------|---|----------------|
| IDEM1 | SNe Ia+ H_0 | $73.37^{+3.63}_{-3.61}$ | $0.354^{+0.109}_{-0.162}$ | $-0.53^{+1.02}_{-0.91}$ | 682.14 |
| | SNe Ia+ H_0 +CC | $70.78^{+3.62}_{-3.61}$ | $0.307^{+0.108}_{-0.122}$ | $-0.07^{+0.58}_{-0.74}$ | 695.45 |
| | SNe Ia+ H_0 +CC+BAO | $69.44^{+3.62}_{-3.61}$ | $0.321^{+0.072}_{-0.078}$ | $-0.06^{+0.16}_{-0.18}$ | 697.77 |
| | Planck TT | $68.13^{+2.86}_{-2.96}$ | $0.3143^{+0.0636}_{-0.0685}$ | $-0.010^{+0.108}_{-0.140}$ | 11261.4 |
| IDEM2 | SNe Ia+ H_0 | $73.29^{+3.60}_{-3.60}$ | $0.371^{+0.189}_{-0.136}$ | $-0.40^{+0.58}_{-0.94}$ | 682.24 |
| | SNe Ia+ H_0 +CC | $69.75^{+3.60}_{-3.60}$ | $0.307^{+0.186}_{-0.148}$ | $-0.04^{+0.60}_{-0.70}$ | 695.46 |
| | SNe Ia+ H_0 +CC+BAO | $69.72^{+3.60}_{-3.60}$ | $0.326^{+0.110}_{-0.104}$ | $-0.08^{+0.28}_{-0.24}$ | 697.81 |
| | Planck TT | $68.00^{+2.28}_{-2.47}$ | $0.3054^{+0.054}_{-0.050}$ | $-0.0024^{+0.104}_{-0.105}$ | 11262.2 |
| IDEM3 | SNe Ia+ H_0 | $73.21^{+3.60}_{-3.60}$ | $0.370^{+0.196}_{-0.136}$ | $-0.23^{+0.23}_{-1.31}$ | 682.22 |
| | SNe Ia+ H_0 +CC | $70.70^{+3.60}_{-3.60}$ | $0.381^{+0.194}_{-0.138}$ | $-0.27^{+0.46}_{-0.31}$ | 682.23 |
| | SNe Ia+ H_0 +CC+BAO | $69.64^{+3.60}_{-3.60}$ | $0.320^{+0.088}_{-0.088}$ | $-0.038^{+0.24}_{-0.22}$ | 697.74 |
| | Planck TT | $67.35^{+2.41}_{-2.00}$ | $0.3157^{+0.0465}_{-0.0641}$ | $(1.36^{+9.62}_{-8.47}) \times 10^{-06}$ | 11262.0 |
| IDEM4 | SNe Ia+ H_0 | $73.21^{+3.60}_{-3.61}$ | $0.379^{+0.097}_{-0.239}$ | $-0.26^{+0.70}_{-0.24}$ | 682.22 |
| | SNe Ia+ H_0 +CC | $70.70^{+4.81}_{-4.82}$ | $0.379^{+0.097}_{-0.238}$ | $-0.27^{+0.68}_{-0.24}$ | 682.24 |
| | SNe Ia+ H_0 +CC+BAO | $69.64^{+3.60}_{-3.61}$ | $0.320^{+0.087}_{-0.089}$ | $-0.037^{+0.22}_{-0.20}$ | 697.75 |
| | Planck TT | $67.51^{+2.47}_{-2.66}$ | $0.309^{+0.058}_{-0.058}$ | $-0.0052^{+0.102}_{-0.098}$ | 11262.1 |
| IDEM5 | SNe Ia+ H_0 | $73.24^{+3.60}_{-3.61}$ | $0.362^{+0.134}_{-0.220}$ | $-0.36^{+0.36}_{-0.60}$ | 682.11 |
| | SNe Ia+ H_0 +CC | $70.05^{+3.60}_{-3.61}$ | $0.307^{+0.080}_{-0.108}$ | $-0.092^{+0.10}_{-0.22}$ | 695.45 |
| | SNe Ia+ H_0 +CC+BAO | $69.56^{+3.60}_{-3.61}$ | $0.309^{+0.026}_{-0.029}$ | $-0.0019^{+0.0070}_{-0.0072}$ | 697.83 |
| | Planck TT | $67.36^{+2.81}_{-2.53}$ | $0.3154^{+0.024}_{-0.030}$ | $(-9.73^{+8.82}_{-8.37}) \times 10^{-05}$ | 11262.2 |

Table 3: Result of the statistical analysis with 2σ CL for all IDEMs.

6. Discussion and Conclusions

We investigated five types of dark-sector interactions for which the ratio r of the energy densities of CDM and DE is a function of the scale factor only. These models are examples of a general class for which a unified description in terms of a function $f(r)$ is possible. Requiring that early DE be not

| Parameters | IDEM 1 | IDEM 2 | IDEM 3 | IDEM 4 | IDEM 5 |
|-------------------|---------------------------------|---------------------------------|---------------------------------|----------------------------------|-------------------------------|
| $\Omega_{b0}h^2$ | $0.02217^{+0.00046}_{-0.00048}$ | $0.02235^{+0.00048}_{-0.00048}$ | $0.02220^{+0.00052}_{-0.00052}$ | $0.022320^{+0.00046}_{-0.00048}$ | $0.02228^{+0.050}_{-0.052}$ |
| $\Omega_{c0}h^2$ | $0.1121^{+0.0200}_{-0.0196}$ | $0.1299^{+0.0240}_{-0.0166}$ | $0.1198^{+0.0068}_{-0.0078}$ | $0.1190^{+0.0190}_{-0.0158}$ | $0.1248^{+0.0070}_{-0.0076}$ |
| $100\theta_s$ | $1.042^{+0.00092}_{-0.00092}$ | $1.042^{+0.00092}_{-0.00092}$ | $1.042^{+0.00090}_{-0.00090}$ | $1.042^{+0.00092}_{-0.00090}$ | $1.042^{+0.00088}_{-0.00082}$ |
| $\ln(10^{10}A_s)$ | $3.073^{+0.076}_{-0.076}$ | $3.086^{+0.074}_{-0.076}$ | $3.069^{+0.068}_{-0.074}$ | $3.095^{+0.074}_{-0.076}$ | $3.073^{+0.072}_{-0.070}$ |
| n_s | $0.9751^{+0.0128}_{-0.0132}$ | $0.9637^{+0.0126}_{-0.0130}$ | $0.9627^{+0.0132}_{-0.0138}$ | $0.9673^{+0.0063}_{-0.0065}$ | $0.9571^{+0.0067}_{-0.0065}$ |
| τ_{reio} | $0.07477^{+0.019}_{-0.020}$ | $0.07585^{+0.019}_{-0.020}$ | $0.06931^{+0.018}_{-0.019}$ | $0.08166^{+0.019}_{-0.020}$ | $0.06573^{+0.019}_{-0.019}$ |

Table 4: Result of the statistical analysis with 2σ CL for all IDEMs using only Planck TT data.

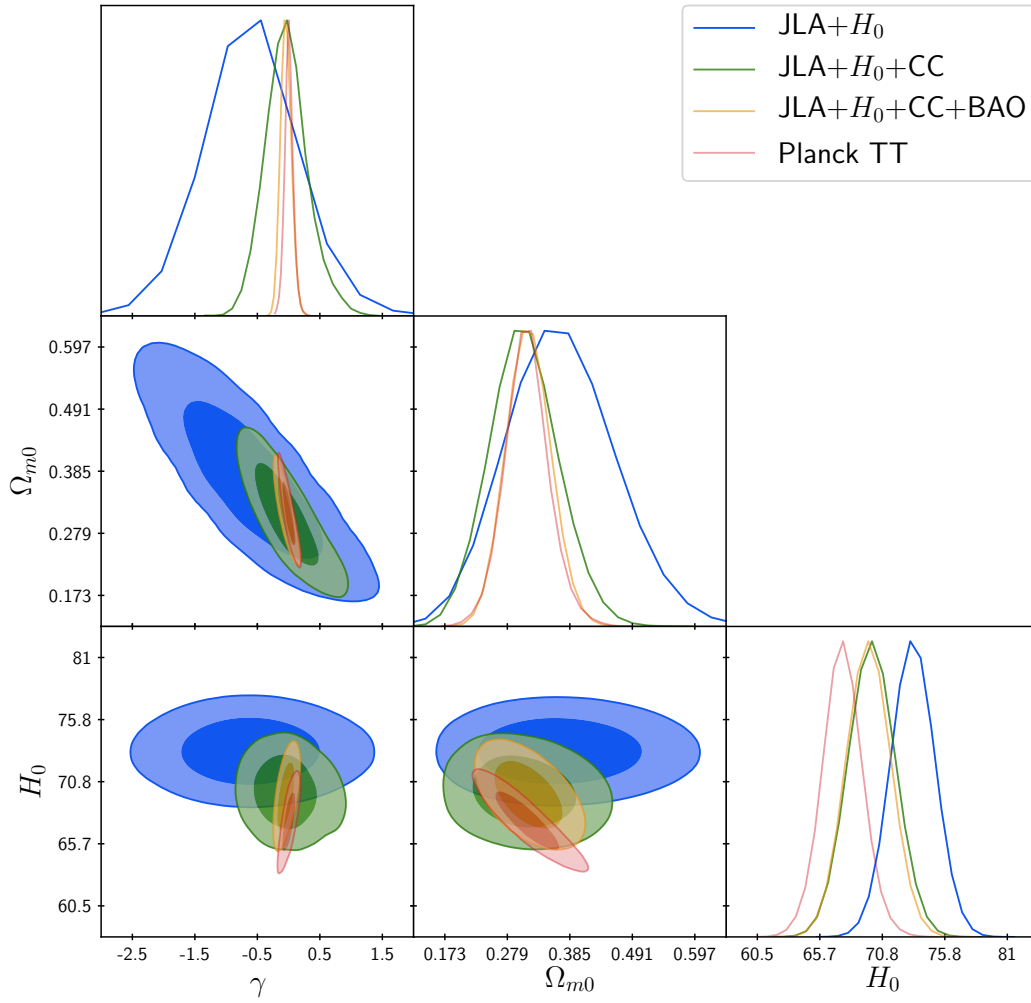


Figure 17: Statistical analysis IDEM 1.

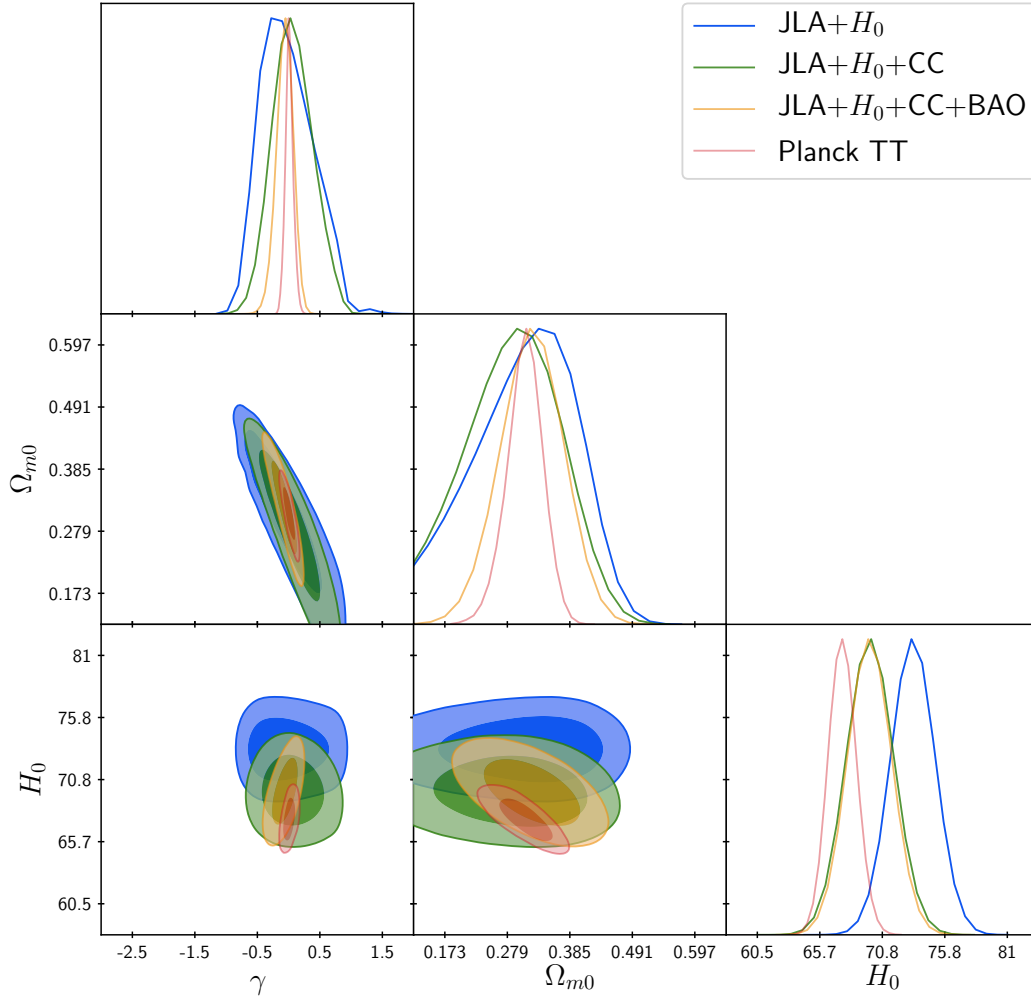


Figure 18: Statistical analysis IDEM 2.

negative provides us with constraints on the interaction parameter γ . For models IDEM 2 and IDEM 4 we have a negative lower bound on γ , while for IDEM 3 and IDEM 5 there is an upper limit $\gamma = 0$, which means that only matter creation is allowed in these models.

Models IDEM 3 and IDEM 5 are particularly sensitive to the interaction, even a small value of the interaction parameter can drastically affect the background dynamics. As shown in Fig.16 the interaction for IDEM 3 and IDEM 5 at high redshift is stronger than that for the other models. This

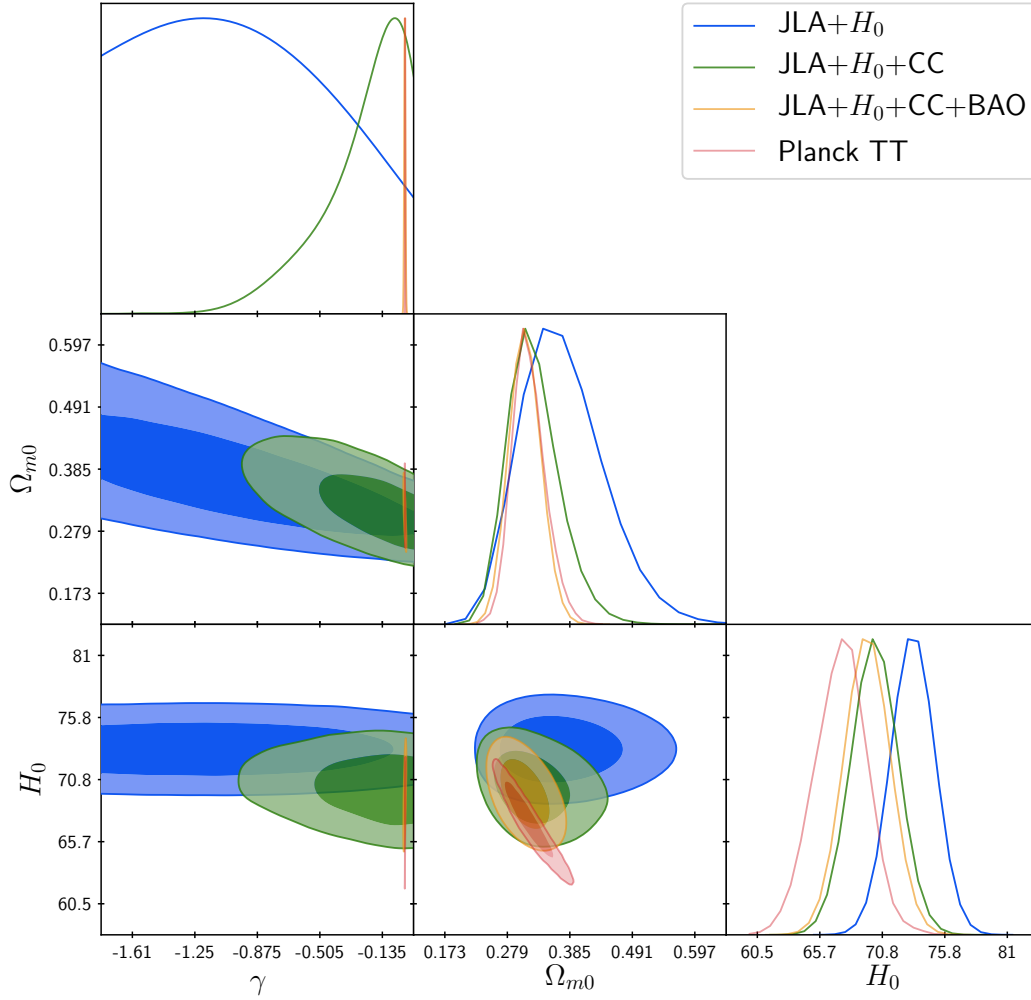


Figure 19: Statistical analysis IDEM 3.

indicates a rather high rate of matter creation at an early epoch. Since we don't expect a present amount of CDM much bigger than the standard-model value, such interacting models necessarily have a rather low CDM fraction in the past. As Figs. 8 and 14 show, these models, upon assuming the standard value of Ω_{c0} , predict a baryon-dominated era, which does not seem to be compatible with the standard description of the Universe before and through the recombination era.

The late-time observational data from H_0 and SNIa leave room for a

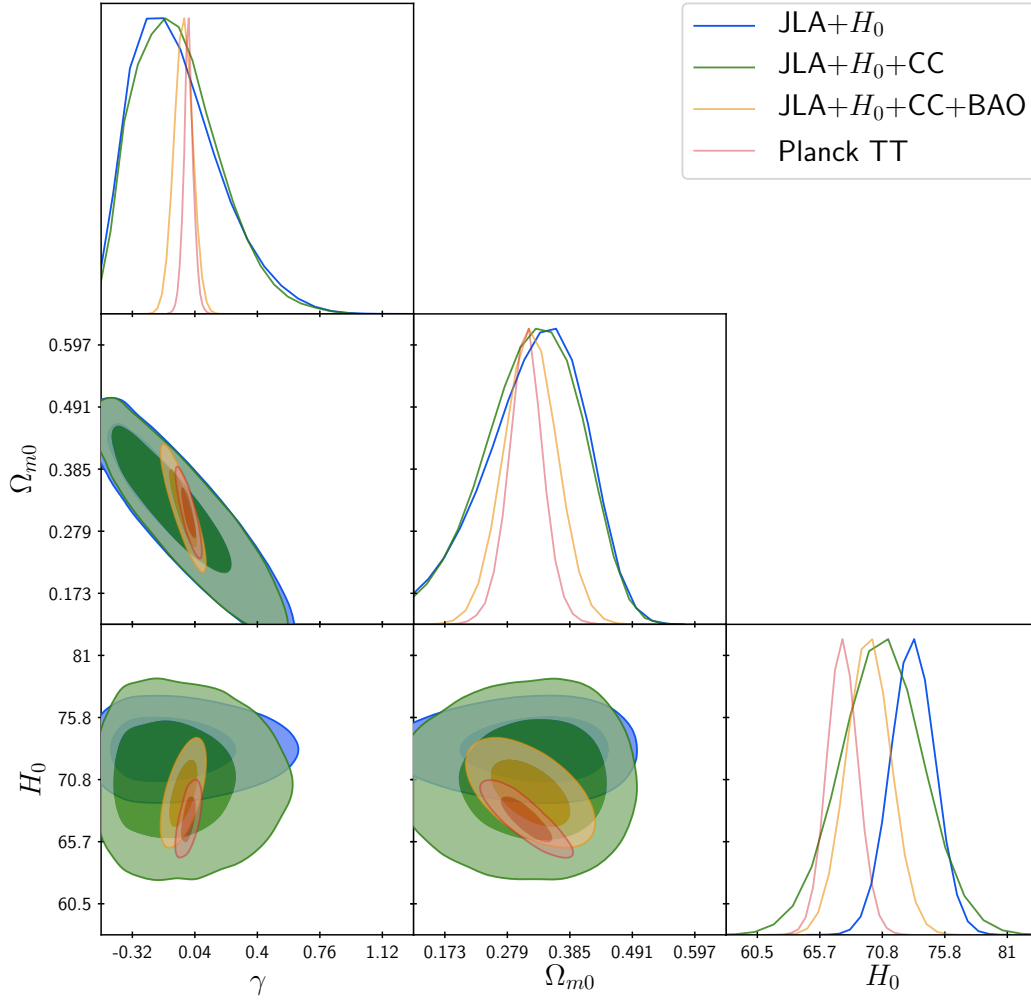


Figure 20: Statistical analysis IDEM 4.

matter creation scenario ($\gamma < 0$). The data from BAO, or above all, from Planck TT, however, constrain the interaction strongly to values very close to $\gamma = 0$ (Λ CDM model). Models IDEM 3 and IDEM 5 are virtually discarded. The remaining models allow for a small range of the interaction parameter ($\gamma \sim \pm 0.15$ at the 2σ confidence level).

Since the Λ CDM model fits most observation extremely well, in particular the CMB data, from the outset, interacting models are not expected to disagree substantially from this standard-model behavior.

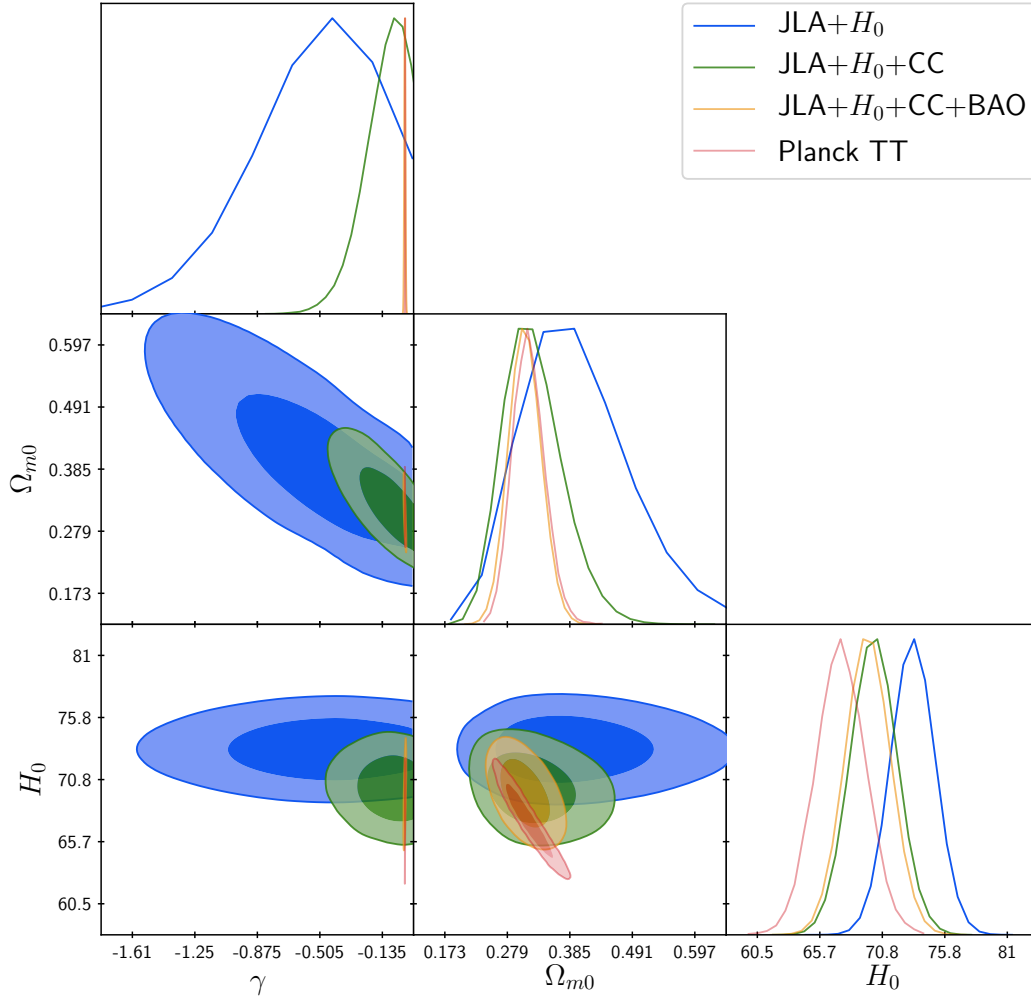


Figure 21: Statistical analysis IDEM 5.

Quite generally, our analysis demonstrates that an interaction in the dark sector is not excluded but the range for the still admissible interaction parameter is very narrow, being always consistent in 1σ CL with the zero coupling case ($\gamma = 0$). Moreover, for viable models the interaction has to become dynamically relevant only close to the present time. An extended analysis of these models (for example at non-linear level) may indicate that even this small interaction can lead to interesting results.

| Model | Ω_{m0} | γ | α | β | Δ_M |
|---------------|---------------------------|----------------------------|------------------------------|---------------------------|-------------------------------|
| Λ CDM | $0.295^{+0.072}_{-0.068}$ | 0 | $0.1412^{+0.0137}_{-0.0133}$ | $3.098^{+0.176}_{-0.156}$ | $-0.0698^{+0.0473}_{-0.0478}$ |
| IDEM1 | $0.365^{+0.188}_{-0.172}$ | $-0.579^{+1.505}_{-2.696}$ | $0.1404^{+0.0143}_{-0.0130}$ | $3.099^{+0.174}_{-0.158}$ | $-0.0703^{+0.0472}_{-0.0479}$ |
| IDEM2 | $0.376^{+0.086}_{-0.267}$ | $-0.400^{+1.192}_{-0.314}$ | $0.1410^{+0.0139}_{-0.0132}$ | $3.100^{+0.172}_{-0.160}$ | $-0.0705^{+0.0476}_{-0.0473}$ |
| IDEM3 | $0.353^{+0.382}_{-0.142}$ | $-0.813^{+0.955}_{-3.615}$ | $0.1410^{+0.0137}_{-0.1355}$ | $3.106^{+0.170}_{-0.165}$ | $-0.0711^{+0.0477}_{-0.0476}$ |
| IDEM4 | $0.380^{+0.095}_{-0.240}$ | $-0.263^{+0.709}_{-0.228}$ | $0.1406^{+0.0142}_{-0.0129}$ | $3.101^{+0.171}_{-0.162}$ | $-0.0703^{+0.0932}_{-0.0480}$ |
| IDEM5 | $0.359^{+0.135}_{-0.168}$ | $-0.356^{+0.942}_{-0.485}$ | $0.1409^{+0.0140}_{-0.0131}$ | $3.103^{+0.168}_{-0.163}$ | $-0.0698^{+0.0410}_{-0.0540}$ |

Table A.5: Statistical analysis with 2σ CL using the SNe Ia (JLA) data for the nuisance parameters.

Appendix A. The SNe Ia (JLA) analysis

The authors of reference [4] mention that the correlation between Ω_{m0} and the nuisance parameters α , β and Δ_M is small for the Λ CDM model. This fact suggest that for models with isotropic luminosity distance which are evolving smoothly with redshift, the binned JLA data can be a reasonable data set to constrain the cosmological parameters. Now, in the context of the present paper, the interaction parameter γ affects the CDM dynamics (as well as the DE dynamics). Therefore, it seems prudent to verify if there is a correlation between γ and the nuisance parameters α , β and Δ_M . In this appendix we present a statistical analysis for all the investigated models using only the SNe Ia (JLA) data. The result is shown in table A.5 and in figure A.22. In this analysis we marginalize numerically over the combination of the parameters M and H_0 . According our results, one can conclude that the nuisance parameters are almost unaffected by the interaction.

Acknowledgement: We thank S.D.P. Vitenti for valuable instructions about numerical issues and useful discussions. Financial support by CNPq, CAPES and FAPES is gratefully acknowledged. The simulations were performed on resources provided by UNINETT Sigma2 – the National Infrastructure for High Performance Computing and Data Storage in Norway. This work has made use of the computing facilities of NPAD/UFRN, and of the Laboratory of Astroinformatics (IAG/USP, NAT/Unicsul), whose purchase was made possible by the Brazilian agency FAPESP (2009/54006-4) and the INCT-A. RvM acknowledges support from Federal Commission for Scholarships for Foreign Students for the Swiss Government Excellence Scholarship (ESKAS No. 2018.0443) for the academic year 2018–2019.

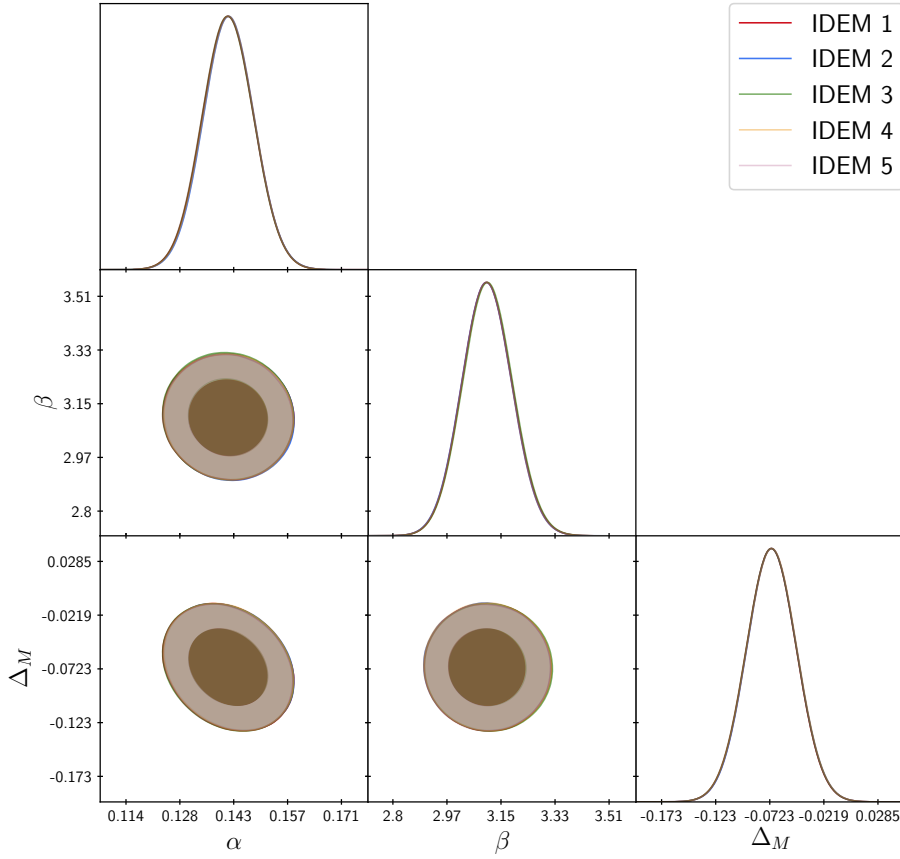


Figure A.22: Statistical analysis using the SNe Ia (JLA) data for the nuisance parameters α , β and Δ_M .

References

- [1] T. M. C. Abbott *et al.*, “Dark Energy Survey Year 1 Results: A Precise H_0 Measurement from DES Y1, BAO, and D/H Data,” 2017.
- [2] P. A. R. Ade *et al.*, “Planck 2015 results. XIII. Cosmological parameters,” *Astron. Astrophys.*, vol. 594, p. A13, 2016.
- [3] P. A. R. Ade *et al.*, “Planck 2015 results. XIV. Dark energy and modified gravity,” *Astron. Astrophys.*, vol. 594, p. A14, 2016.
- [4] M. Betoule *et al.*, “Improved cosmological constraints from a joint anal-

- ysis of the SDSS-II and SNLS supernova samples,” *Astron. Astrophys.*, vol. 568, p. A22, 2014.
- [5] M. Kowalski *et al.*, “Improved Cosmological Constraints from New, Old and Combined Supernova Datasets,” *Astrophys. J.*, vol. 686, pp. 749–778, 2008.
- [6] M. Hicken, W. M. Wood-Vasey, S. Blondin, P. Challis, S. Jha, P. L. Kelly, A. Rest, and R. P. Kirshner, “Improved Dark Energy Constraints from 100 New CfA Supernova Type Ia Light Curves,” *Astrophys. J.*, vol. 700, pp. 1097–1140, 2009.
- [7] R. Amanullah *et al.*, “Spectra and Light Curves of Six Type Ia Supernovae at $0.511 < z < 1.12$ and the Union2 Compilation,” *Astrophys. J.*, vol. 716, pp. 712–738, 2010.
- [8] N. Suzuki *et al.*, “The Hubble Space Telescope Cluster Supernova Survey: V. Improving the Dark Energy Constraints Above $z > 1$ and Building an Early-Type-Hosted Supernova Sample,” *Astrophys. J.*, vol. 746, p. 85, 2012.
- [9] G. Hinshaw *et al.*, “Nine-Year Wilkinson Microwave Anisotropy Probe (WMAP) Observations: Cosmological Parameter Results,” *Astrophys. J. Suppl.*, vol. 208, p. 19, 2013.
- [10] F. Zwicky, “Die Rotverschiebung von extragalaktischen Nebeln,” *Helv. Phys. Acta*, vol. 6, pp. 110–127, 1933. [Gen. Rel. Grav.41,207(2009)].
- [11] Y. Sofue and V. Rubin, “Rotation curves of spiral galaxies,” *Ann. Rev. Astron. Astrophys.*, vol. 39, pp. 137–174, 2001.
- [12] A. G. Riess *et al.*, “Observational evidence from supernovae for an accelerating universe and a cosmological constant,” *Astron. J.*, vol. 116, pp. 1009–1038, 1998.
- [13] S. Perlmutter *et al.*, “Measurements of Omega and Lambda from 42 high redshift supernovae,” *Astrophys. J.*, vol. 517, pp. 565–586, 1999.
- [14] S. Weinberg, “The Cosmological Constant Problem,” *Rev. Mod. Phys.*, vol. 61, pp. 1–23, 1989.

- [15] M. Chevallier and D. Polarski, “Accelerating universes with scaling dark matter,” *Int. J. Mod. Phys.*, vol. D10, pp. 213–224, 2001.
- [16] E. V. Linder, “Exploring the expansion history of the universe,” *Phys. Rev. Lett.*, vol. 90, p. 091301, 2003.
- [17] R. R. Caldwell, R. Dave, and P. J. Steinhardt, “Cosmological imprint of an energy component with general equation of state,” *Phys. Rev. Lett.*, vol. 80, pp. 1582–1585, 1998.
- [18] C. Armendariz-Picon, V. F. Mukhanov, and P. J. Steinhardt, “Essentials of k essence,” *Phys. Rev.*, vol. D63, p. 103510, 2001.
- [19] T. Clifton, P. G. Ferreira, A. Padilla, and C. Skordis, “Modified Gravity and Cosmology,” *Phys. Rept.*, vol. 513, pp. 1–189, 2012.
- [20] A. Joyce, B. Jain, J. Khoury, and M. Trodden, “Beyond the Cosmological Standard Model,” *Phys. Rept.*, vol. 568, pp. 1–98, 2015.
- [21] A. P. Billyard and A. A. Coley, “Interactions in scalar field cosmology,” *Phys. Rev.*, vol. D61, p. 083503, 2000.
- [22] L. Amendola, “Coupled quintessence,” *Phys. Rev.*, vol. D62, p. 043511, 2000.
- [23] W. Zimdahl, D. Pavon, and L. P. Chimento, “Interacting quintessence,” *Phys. Lett.*, vol. B521, pp. 133–138, 2001.
- [24] L. P. Chimento, A. S. Jakubi, D. Pavon, and W. Zimdahl, “Interacting quintessence solution to the coincidence problem,” *Phys. Rev.*, vol. D67, p. 083513, 2003.
- [25] J.-H. He and B. Wang, “Effects of the interaction between dark energy and dark matter on cosmological parameters,” *JCAP*, vol. 0806, p. 010, 2008.
- [26] J. Valiviita, E. Majerotto, and R. Maartens, “Instability in interacting dark energy and dark matter fluids,” *JCAP*, vol. 0807, p. 020, 2008.
- [27] T. Clemson, K. Koyama, G.-B. Zhao, R. Maartens, and J. Valiviita, “Interacting Dark Energy – constraints and degeneracies,” *Phys. Rev.*, vol. D85, p. 043007, 2012.

- [28] Y.-H. Li, J.-F. Zhang, and X. Zhang, “Parametrized Post-Friedmann Framework for Interacting Dark Energy,” *Phys. Rev.*, vol. D90, no. 6, p. 063005, 2014.
- [29] C. Skordis, D. F. Mota, P. G. Ferreira, and C. Boehm, “Large Scale Structure in Bekenstein’s theory of relativistic Modified Newtonian Dynamics,” *Phys. Rev. Lett.*, vol. 96, p. 011301, 2006.
- [30] Y. Akrami, T. S. Koivisto, D. F. Mota, and M. Sandstad, “Bimetric gravity doubly coupled to matter: theory and cosmological implications,” *JCAP*, vol. 1310, p. 046, 2013.
- [31] J. D. Barrow and D. F. Mota, “Gauge invariant perturbations of varying alpha cosmologies,” *Class. Quant. Grav.*, vol. 20, pp. 2045–2062, 2003.
- [32] V. Faraoni, J. B. Dent, and E. N. Saridakis, “Covariantizing the interaction between dark energy and dark matter,” *Phys. Rev.*, vol. D90, no. 6, p. 063510, 2014.
- [33] V. Marra, “Coupling dark energy to dark matter inhomogeneities,” *Phys. Dark Univ.*, vol. 13, pp. 25–29, 2016.
- [34] I. Odderskov, M. Baldi, and L. Amendola, “The effect of interacting dark energy on local measurements of the Hubble constant,” *JCAP*, vol. 1605, no. 05, p. 035, 2016.
- [35] B. Wang, E. Abdalla, F. Atrio-Barandela, and D. Pavon, “Dark Matter and Dark Energy Interactions: Theoretical Challenges, Cosmological Implications and Observational Signatures,” *Rept. Prog. Phys.*, vol. 79, no. 9, p. 096901, 2016.
- [36] R. F. vom Marttens, L. Casarini, W. S. Hipólito-Ricaldi, and W. Zimdahl, “CMB and matter power spectra with non-linear dark-sector interactions,” *JCAP*, vol. 1701, no. 01, p. 050, 2017.
- [37] F. Arevalo, A. Cid, and J. Moya, “AIC and BIC for cosmological interacting scenarios,” *Eur. Phys. J.*, vol. C77, no. 8, p. 565, 2017.
- [38] S. Kumar and R. C. Nunes, “Echo of interactions in the dark sector,” *Phys. Rev.*, vol. D96, no. 10, p. 103511, 2017.

- [39] J. E. Gonzalez, H. H. B. Silva, R. Silva, and J. S. Alcaniz, “Physical constraints on interacting dark energy models,” *Eur. Phys. J.*, vol. C78, no. 9, p. 730, 2018.
- [40] S. Das, P. S. Corasaniti, and J. Khoury, “Super-acceleration as signature of dark sector interaction,” *Phys. Rev.*, vol. D73, p. 083509, 2006.
- [41] E. G. M. Ferreira, J. Quintin, A. A. Costa, E. Abdalla, and B. Wang, “Evidence for interacting dark energy from BOSS,” *Phys. Rev.*, vol. D95, no. 4, p. 043520, 2017.
- [42] C.-G. Park, J.-c. Hwang, J.-h. Lee, and H. Noh, “Roles of dark energy perturbations in the dynamical dark energy models: Can we ignore them?,” *Phys. Rev. Lett.*, vol. 103, p. 151303, 2009.
- [43] L. Santos, W. Zhao, E. G. M. Ferreira, and J. Quintin, “Constraining interacting dark energy with CMB and BAO future surveys,” *Phys. Rev.*, vol. D96, no. 10, p. 103529, 2017.
- [44] J. Mifsud and C. Van De Bruck, “Probing the imprints of generalized interacting dark energy on the growth of perturbations,” *JCAP*, vol. 1711, no. 11, p. 001, 2017.
- [45] A. Gomez-Valent and J. Sola, “Relaxing the σ_8 -tension through running vacuum in the Universe,” 2017.
- [46] J. Sola, “Cosmologies with a time dependent vacuum,” *J. Phys. Conf. Ser.*, vol. 283, p. 012033, 2011.
- [47] A. A. Costa, X.-D. Xu, B. Wang, and E. Abdalla, “Constraints on interacting dark energy models from Planck 2015 and redshift-space distortion data,” *JCAP*, vol. 1701, no. 01, p. 028, 2017.
- [48] A. G. Riess, L. Macri, S. Casertano, H. Lampeitl, H. C. Ferguson, A. V. Filippenko, S. W. Jha, W. Li, and R. Chornock, “A 3% Solution: Determination of the Hubble Constant with the Hubble Space Telescope and Wide Field Camera 3,” *Astrophys. J.*, vol. 730, p. 119, 2011. [Erratum: *Astrophys. J.*732,129(2011)].
- [49] F. Beutler, C. Blake, M. Colless, D. H. Jones, L. Staveley-Smith, L. Campbell, Q. Parker, W. Saunders, and F. Watson, “The 6dF Galaxy

- Survey: Baryon Acoustic Oscillations and the Local Hubble Constant,” *Mon. Not. Roy. Astron. Soc.*, vol. 416, pp. 3017–3032, 2011.
- [50] A. J. Ross, L. Samushia, C. Howlett, W. J. Percival, A. Burden, and M. Manera, “The clustering of the SDSS DR7 main Galaxy sample – I. A 4 per cent distance measure at $z = 0.15$,” *Mon. Not. Roy. Astron. Soc.*, vol. 449, no. 1, pp. 835–847, 2015.
- [51] L. Anderson *et al.*, “The clustering of galaxies in the SDSS-III Baryon Oscillation Spectroscopic Survey: baryon acoustic oscillations in the Data Releases 10 and 11 Galaxy samples,” *Mon. Not. Roy. Astron. Soc.*, vol. 441, no. 1, pp. 24–62, 2014.
- [52] S. Alam *et al.*, “The clustering of galaxies in the completed SDSS-III Baryon Oscillation Spectroscopic Survey: cosmological analysis of the DR12 galaxy sample,” *Mon. Not. Roy. Astron. Soc.*, vol. 470, no. 3, pp. 2617–2652, 2017.
- [53] E. A. Kazin *et al.*, “The WiggleZ Dark Energy Survey: improved distance measurements to $z = 1$ with reconstruction of the baryonic acoustic feature,” *Mon. Not. Roy. Astron. Soc.*, vol. 441, no. 4, pp. 3524–3542, 2014.
- [54] H. E. S. Velten, R. F. vom Marttens, and W. Zimdahl, “Aspects of the cosmological “coincidence problem”,” *Eur. Phys. J.*, vol. C74, no. 11, p. 3160, 2014.
- [55] W. Zimdahl, D. Pavon, L. P. Chimento, and A. S. Jakubi, “Interacting quintessence and the coincidence problem,” in *On recent developments in theoretical and experimental general relativity, gravitation, and relativistic field theories. Proceedings, 10th Marcel Grossmann Meeting, MG10, Rio de Janeiro, Brazil, July 20-26, 2003. Pt. A-C*, pp. 1794–1796, 2004.
- [56] K. Nozari, N. Behrouz, and N. Rashidi, “Interaction between Dark Matter and Dark Energy and the Cosmological Coincidence Problem,” *Adv. High Energy Phys.*, vol. 2014, p. 569702, 2014.
- [57] W. Yang, S. Pan, and J. D. Barrow, “Large-scale Stability and Astronomical Constraints for Coupled Dark-Energy Models,” 2017.

- [58] W. Yang, S. Pan, and D. F. Mota, “Novel approach toward the large-scale stable interacting dark-energy models and their astronomical bounds,” *Phys. Rev.*, vol. D96, no. 12, p. 123508, 2017.
- [59] W. Yang, S. Pan, E. Di Valentino, R. C. Nunes, S. Vagnozzi, and D. F. Mota, “Tale of stable interacting dark energy, observational signatures, and the H_0 tension,” 2018.
- [60] L. P. Chimento, M. I. Forte, and G. M. Kremer, “Cosmological model with interactions in the dark sector,” *Gen. Rel. Grav.*, vol. 41, pp. 1125–1137, 2009.
- [61] C.-P. Ma and E. Bertschinger, “Cosmological perturbation theory in the synchronous and conformal Newtonian gauges,” *Astrophys. J.*, vol. 455, pp. 7–25, 1995.
- [62] G. Caldera-Cabral, R. Maartens, and B. M. Schaefer, “The Growth of Structure in Interacting Dark Energy Models,” *JCAP*, vol. 0907, p. 027, 2009.
- [63] E. Majerotto, J. Valiviita, and R. Maartens, “Adiabatic initial conditions for perturbations in interacting dark energy models,” *Mon. Not. Roy. Astron. Soc.*, vol. 402, pp. 2344–2354, 2010.
- [64] H. Velten, R. E. Fazolo, R. von Marttens, and S. Gomes, “Degeneracy between nonadiabatic dark energy models and Λ CDM: ISW effect and the cross correlation of CMB with galaxy clustering data,” 2018.
- [65] Y. Wang, D. Wands, L. Xu, J. De-Santiago, and A. Hojjati, “Cosmological constraints on a decomposed Chaplygin gas,” *Phys. Rev.*, vol. D87, no. 8, p. 083503, 2013.
- [66] L. Amendola, F. Finelli, C. Burigana, and D. Carturan, “WMAP and the generalized Chaplygin gas,” *JCAP*, vol. 0307, p. 005, 2003.
- [67] R. F. vom Marttens, L. Casarini, W. Zimdahl, W. S. Hipólito-Ricaldi, and D. F. Mota, “Does a generalized Chaplygin gas correctly describe the cosmological dark sector?,” *Phys. Dark Univ.*, vol. 15, pp. 114–124, 2017.

- [68] A. R. Fuño, W. S. Hipólito-Ricaldi, and W. Zimdahl, “Matter Perturbations in Scaling Cosmology,” *Mon. Not. Roy. Astron. Soc.*, vol. 457, no. 3, pp. 2958–2967, 2016.
- [69] F. Arevalo, A. P. R. Bacalhau, and W. Zimdahl, “Cosmological dynamics with non-linear interactions,” *Class. Quant. Grav.*, vol. 29, p. 235001, 2012.
- [70] D. Blas, J. Lesgourgues, and T. Tram, “The Cosmic Linear Anisotropy Solving System (CLASS) II: Approximation schemes,” *JCAP*, vol. 1107, p. 034, 2011.
- [71] B. Audren, J. Lesgourgues, K. Benabed, and S. Prunet, “Conservative Constraints on Early Cosmology: an illustration of the Monte Python cosmological parameter inference code,” *JCAP*, vol. 1302, p. 001, 2013.
- [72] T. Brinckmann and J. Lesgourgues, “MontePython 3: boosted MCMC sampler and other features,” 2018.
- [73] A. G. Riess *et al.*, “A 2.4% Determination of the Local Value of the Hubble Constant,” *Astrophys. J.*, vol. 826, no. 1, p. 56, 2016.
- [74] C. Zhang, H. Zhang, S. Yuan, T.-J. Zhang, and Y.-C. Sun, “Four new observational $H(z)$ data from luminous red galaxies in the Sloan Digital Sky Survey data release seven,” *Res. Astron. Astrophys.*, vol. 14, no. 10, pp. 1221–1233, 2014.
- [75] J. Simon, L. Verde, and R. Jimenez, “Constraints on the redshift dependence of the dark energy potential,” *Phys. Rev.*, vol. D71, p. 123001, 2005.
- [76] M. Moresco *et al.*, “Improved constraints on the expansion rate of the Universe up to z 1.1 from the spectroscopic evolution of cosmic chronometers,” *JCAP*, vol. 1208, p. 006, 2012.
- [77] M. Moresco, L. Pozzetti, A. Cimatti, R. Jimenez, C. Maraston, L. Verde, D. Thomas, A. Citro, R. Tojeiro, and D. Wilkinson, “A 6% measurement of the Hubble parameter at $z \sim 0.45$: direct evidence of the epoch of cosmic re-acceleration,” *JCAP*, vol. 1605, no. 05, p. 014, 2016.

- [78] D. Stern, R. Jimenez, L. Verde, M. Kamionkowski, and S. A. Stanford, “Cosmic Chronometers: Constraining the Equation of State of Dark Energy. I: $H(z)$ Measurements,” *JCAP*, vol. 1002, p. 008, 2010.
- [79] A. L. Ratsimbazafy, S. I. Loubser, S. M. Crawford, C. M. Cress, B. A. Bassett, R. C. Nichol, and P. Väisänen, “Age-dating Luminous Red Galaxies observed with the Southern African Large Telescope,” *Mon. Not. Roy. Astron. Soc.*, vol. 467, no. 3, pp. 3239–3254, 2017.
- [80] M. Moresco, “Raising the bar: new constraints on the Hubble parameter with cosmic chronometers at $z \sim 2$,” *Mon. Not. Roy. Astron. Soc.*, vol. 450, no. 1, pp. L16–L20, 2015.
- [81] A. Cid, B. Santos, C. Pigozzo, T. Ferreira, and J. Alcaniz, “Bayesian Comparison of Interacting Scenarios,” 2018.
- [82] N. Aghanim *et al.*, “Planck 2015 results. XI. CMB power spectra, likelihoods, and robustness of parameters,” *Astron. Astrophys.*, vol. 594, p. A11, 2016.
- [83] M. Pettini and R. Cooke, “A new, precise measurement of the primordial abundance of Deuterium,” *Mon. Not. Roy. Astron. Soc.*, vol. 425, pp. 2477–2486, 2012.
- [84] A. Gelman and D. B. Rubin, “Inference from Iterative Simulation Using Multiple Sequences,” *Statist. Sci.*, vol. 7, pp. 457–472, 1992.